Computational Studies of Dispersion Interactions in Coinage and Volatile Metal Clusters

Richard Hatz

University of Helsinki
Faculty of Science
Department of Chemistry
Laboratory of Physical Chemistry
A.I. Virtasen aukio 1 (P.O. BOX 55)
FI-00014 University of Helsinki, Finland

Academic Dissertation

To be presented, with the permission of the Faculty of Science of the University of Helsinki, for public discussion in Auditorium A110, Department of Chemistry (A.I. Virtasen aukio 1, Helsinki), on March 18, 2016 at 12 o'clock.

Helsinki 2016

Supervised by:

Prof. Lauri Halonen
Department of Chemistry
University of Helsinki
Helsinki, Finland

Dr. Vesa Hänninen
Department of Chemistry
University of Helsinki
Helsinki, Finland

Reviewed by:

Prof. Juha Vaara
Department of Physics
University of Oulu
Oulu, Finland

Prof. Emer. Matti Hotokka
Laboratory of Physical Chemistry
Åbo Akademi University
Turku, Finland

Opponent:

Prof. Emer. Ad van der Avoird
Institute for Molecules and Materials
Radboud University Nijmegen
Nijmegen, The Netherlands

Custos:

Prof. Lauri Halonen
Department of Chemistry
University of Helsinki
Helsinki, Finland

ISBN 978-951-51-1908-7 (paperback)
ISBN 978-951-51-1909-4 (PDF)
`http://ethesis.helsinki.fi`
Unigrafia Helsinki 2016

Abstract

Intermolecular interactions are ubiquitous, and their intricate network plays a decisive role in most of the phenomena encountered in our everyday lives. The focus of this thesis is on the London dispersion forces, a component present in all interactions between atoms and molecules, and often the most important one at long intermolecular distances. The quantum-mechanical origin of these forces can be traced to the correlated fluctuations of the molecular charge distributions, which however render the dispersion interactions challenging to calculate accurately, due to the high-level electronic structure methods required. The aim of the research presented in this thesis is to investigate the dispersion interactions, and to develop a viable method for modeling them.

The systems studied in the accompanying research articles mainly encompass small clusters of coinage (Cu, Ag, and Au) and volatile (Zn, Cd, and Hg) metals. The long-range forces present in these clusters are calculated by means of highly correlated electronic structure methods, and the interaction potentials are used to develop a simple but effective model, capable of accurately describing the dispersion interactions in a variety of systems. Some original theoretical considerations are also elaborated. A novel formula is derived for the tensor describing all intermolecular interactions, and it is applied to investigate the long-range interaction potential of coinage metal–hydrogen clusters.

The method developed to account for the dispersion energy is a pair-potential model, where the total intermolecular London forces are calculated by means of atomic dispersion coefficients describing the magnitude and orientation dependence of the interaction. The coefficients are calculated based on small model systems, and they are used to compute the dispersion energy in larger clusters at no additional cost. Encouraging results are also obtained for the computed orientation averaged interaction potentials. All things considered, the publications included in this thesis indicate that the methods proposed and implemented to analyze the studied systems are capable of accurately modeling the non-covalent forces in a straightforward fashion.

List of Publications

List of Publications Included in the Thesis

I Hatz, R.; Korpinen, M.; Hänninen, V.; Halonen, L. Characterization of the Dispersion Interactions and an ab Initio Study of van der Waals Potential Energy Parameters for Coinage Metal Clusters. *J. Phys. Chem. A* **2012**, *116*, 11685–11693, DOI: 10.1021/jp307448n

II Hatz, R.; Hänninen, V.; Halonen, L. Dispersion Interactions in Small Zinc, Cadmium, and Mercury Clusters. *J. Phys. Chem. A* **2014**, *118*, 5734–5740, DOI: 10.1021/jp505023g

III Hatz, R.; Hänninen, V.; Halonen, L. Pair-Potential Approach to Accurate Dispersion Energies between Group 12 (Zn, Cd, Hg) Clusters. *J. Phys. Chem. A* **2014**, *118*, 12274–12279, DOI: 10.1021/jp510622u

IV Hatz, R.; Korpinen, M.; Hänninen, V.; Halonen, L. Generalized Intermolecular Interaction Tensor Applied to Long-Range Interactions in Hydrogen and Coinage Metal (Cu, Ag, and Au) Clusters. *J. Phys. Chem. A* **2015**, *119*, 11729–11736, DOI: 10.1021/acs.jpca.5b09080

In Article I, Richard Hatz performed all of the quantum-chemical computations and data analysis relating to the dispersion coefficients and the finite field calculations of electric properties. In Article II, the doctoral candidate was responsible for all electronic structure calculations, along with the data analysis and theoretical work. The quantum-theoretic computations and data analysis of Article III, as well as the comparisons to other dispersion correction methods and pair-potential models were mostly carried out by the candidate. Richard Hatz derived all theoretical results of Article IV, and performed most of the data analysis to recover the long-range intermolecular interaction parameters. All manuscripts, supporting information, and responses to the comments of the reviewers were written by Richard Hatz. The texts were subsequently finalized as team work.

Acknowledgements

After over two decades of formal education, I am finally about to receive one of the highest academic degrees in our society. In some respects, this is the end of a long journey, but at the same time the beginning of an even longer one. I can only hope that the road ahead brings as much delight and joy of scientific discovery as the one leading upto it.

Although my name is the only one on the cover, this research would not have been possible without the efforts and support of several people. First and foremost I wish to express my gratitude towards professor Lauri Halonen, without whom this thesis would never have become into existence. Thank you for believing in me enough to invest the time and resources necessary for the completion of this work. I am grateful to both of my supervisors for your valuable insight and support you have provided me during these years. I also wish to acknowledge my former colleague, Markus Korpinen, for his cooperation and contributions to this study.

Even the life of a quantum chemist is not concentrated solely on numbers and molecules: pleasant people and an encouraging working environment make all the difference. During my time at the University of Helsinki, I have had the pleasure to work with many extraordinary individuals, who have made the laboratory of physical chemistry an enjoyable place to work. When I started to work here, my former roommates Teemu Salmi, Elina Sjöholm, and Salla Tapio all made me feel like a member of a collective family. I would like to thank my colleague Sergio Losilla for his friendship and professional advice. I am also equally thankful to all my other friends, roommates and colleagues, especially Wen Chen, Heike Fliegl, Hannu Koskenvaara, Theo Kurtén, Markus Metsälä, Pauli Parkkinen, Lauri Partanen, Jari Peltola, Janne Pesonen, Matej Pipíška, Matti Rissanen, Mirva Skyttä, Ville Ulvila, and Nergiz Özcan-Ketola for all the fun times we have had together.

My final thanks go to my family, who always encouraged me to study and to reach for the stars, and to my better half Elina, who has stood by me and supported me during all these years. Thank you all.

Helsinki, January 19, 2016

Contents

Abstract **i**

List of Publications **ii**

Acknowledgements **iii**

1 Introduction **1**

2 Electronic Structure Theory **3**
2.1 Schrödinger Equation . . . 3
2.2 Hartree–Fock Method . . . 4
2.3 Electron Correlation Methods . . . 5
2.4 Basis Sets . . . 7

3 Intermolecular Interactions **8**
3.1 Coulombic Interactions . . . 8
3.2 Perturbative Multipole Expansion . . . 14
3.3 Electrostatic Interaction . . . 16
3.4 Induction Interaction . . . 18
3.5 Dispersion Interaction . . . 18

4 Results **21**
4.1 Studied Systems . . . 21
4.2 Theoretical Model . . . 23
4.3 Intermolecular Interaction Tensor . . . 25
4.4 Multipole Moments and Polarizabilities . . . 27
4.5 Dispersion Interactions . . . 28
4.6 Applications . . . 33

5 Conclusions **38**

Bibliography **40**

Chapter 1

Introduction

> Nonideal gases taught us a general truth:
> *Electrically neutral bodies attract.*
>
> V. Adrian Parsegian
> *Van der Waals Forces*

Nature provides many examples of the importance of van der Waals (vdW) forces:[1] they help certain lizards and spiders to adhere to smooth surfaces,[2–5] and trigger the coagulation of small interstellar dust particles that eventually form celestial bodies.[6] At the microscopic level, they play an essential role in a myriad of phenomena such as the stability of molecular solids and layered materials,[7–10] or the double-helical structure of DNA.[11–14] These weak long-range intermolecular forces result from the permanent or transient distortions in the molecular electric charge distributions.[15] The most important contribution[16] generally stems from the London dispersion interaction,[17] which derives from the spontaneous correlated fluctuations in the electron densities of the constituent molecules. Due to the Heisenberg uncertainty principle, these fluctuations of quantum-mechanical origin are present in all molecules.[15] Dispersion effects thus constitute a ubiquitous component of intermolecular forces, and dominate the interaction of nonpolar molecules, permitting substances such as noble gases to exist in the solid or liquid state.

Dispersion forces are difficult to quantify experimentally: although direct measurements utilizing Rydberg atoms are possible,[18] the vdW interaction is too small to be explicitly detected between two ground state atoms.[19] This renders theoretical calculations and predictions crucial for the determination of long-range forces. However, as an electron correlation effect, dispersion interactions require advanced electronic structure calculations in order to be accurately modeled. Some rudimentary methods even completely ignore the London forces,[20–24] which introduces problems for large systems, where elaborate calculations are unfeasible.

Several different approximations and methods of computation[25–34] have been developed for the dispersion interactions since the seminal work of London.[17] These range from simple experimental formulas to intricate *a posteriori* corrections, and various explicit *ab initio* methods, able to resolve the vdW dispersion forces with varying degrees of accuracy and computational cost. However, a common source of difficulties is that the strength of the interaction varies with the orientation and size of the constituent molecules, and this anisotropy and inconstant nature of the interactions often induces inaccuracies and increases the computational demands necessary to properly account for them.

In this thesis, the computational and theoretical aspects of dispersion and other intermolecular forces are examined. The studied systems encompass small coinage

and volatile metal clusters, the interactions of which are analyzed via high-level electronic structure calculations, and some novel theoretical considerations. The elements at the focal point of investigation, i.e., the group 11 (Cu, Ag, Au) and group 12 (Zn, Cd, Hg) metals, are intricately connected with dispersion interactions in a particularly interesting fashion. The former group has epitomized the concept of metallophilic interactions,[35–39] the unusually strong van der Waals dispersion forces caused by relativistic effects, first discovered in coinage metal clusters. The volatile metals, on the other hand, provide an exceptional and important field of research due to their bonding, which changes with increasing cluster size from dispersion driven to covalent and ultimately metallic.[40–45] It is therefore evident that long-range interactions are indispensable for the proper description of the chemistry of these metals.

The purpose of this research is to develop a simple but accurate model for dispersion interactions, which could also be used to include these forces in larger systems, decreasing the required computational costs. The scheme presented in this thesis for the computation of the van der Waals interactions is based on an atomic pair dispersion potential model. Accurate *ab initio* methods are utilized to calculate the potential energy surfaces of the studied metal clusters at long intermolecular distances, and the total interaction energy is divided into contributions arising from dispersion, electrostatic, and induction effects. The pair-potential model is least-squares fitted to the total dispersion energy to recover a set of interatomic coefficients describing the interaction. The properties of these vdW parameters are studied, and they are used to reliably model the dispersion effects in various metal clusters. Encouraging results are also obtained for orientation averaged dispersion energies. On the whole, the obtained results indicate that the procedure described is able to accurately account for the non-covalent interactions present in the studied coinage and volatile metal systems.

Some novel theoretical contributions for the description of intermolecular forces are also presented in this thesis. A combinatorial equation is derived for the tensor governing the long-range interaction potential between molecules, and it is utilized to study the dispersion interactions in clusters composed of coinage metal and hydrogen dimers. Several examples are also provided for other possible applications of the presented formulation, which is simple to use, but general enough to encompass arbitrary long-range intermolecular interactions.

This thesis is organized in the following fashion. Chapter 2 provides an overview of the electronic structure methods used in this thesis, while Chapter 3 focuses more closely on the theoretical aspects of intermolecular interactions. The results obtained are summarized in Chapter 4, and the concluding remarks are presented in the final chapter.

Chapter 2

Electronic Structure Theory

Electronic structure theory—the pith of computational chemistry—is an integral part of this thesis. The current chapter provides an overview of the methods used to probe the intermolecular interaction energy, on which all further calculations of the dispersion interactions are based.

2.1 Schrödinger Equation

The behavior of a quantum-mechanical system of non-relativistic particles in time-independent potentials is governed by the Schrödinger equation

$$\hat{H}\Psi = E\Psi, \tag{2.1}$$

which gives the total energy E of the system as the eigenvalue of the Hamiltonian operator $\hat{H}$. The corresponding eigenfunction Ψ is called the wave function, and it contains all possible information about the quantum state it describes. In atomic units* (a.u.), the Hamiltonian of a system composed of electrons and nuclei is

$$\hat{H} = -\frac{1}{2}\sum_i \nabla_i^2 - \frac{1}{2}\sum_A \frac{\nabla_A^2}{m_A} + \sum_{i>j} \frac{1}{|\mathbf{r}_i - \mathbf{r}_j|} + \sum_{A>B} \frac{Z_A Z_B}{|\mathbf{R}_A - \mathbf{R}_B|} - \sum_{i,A} \frac{Z_A}{|\mathbf{r}_i - \mathbf{R}_A|}, \tag{2.2}$$

where the indices i and j run over the electrons, and A and B over the nuclei. The mass and charge of a nucleus are indicated by m and Z, while the positions of the nuclei and electrons are denoted by $\mathbf{R}$ and $\mathbf{r}$, respectively. The terms of the Hamiltonian describe the kinetic and potential energies of the particles, and eq. (2.2) can also be written as

$$\hat{H} = \hat{T}_\mathrm{e} + \hat{T}_\mathrm{N} + \hat{V}_\mathrm{e,e} + \hat{V}_\mathrm{N,N} + \hat{V}_\mathrm{N,e}, \tag{2.3}$$

where $\hat{T}$ and $\hat{V}$ are the operators for kinetic and potential energies, and the indices e and N refer to electrons and nuclei, respectively.

In general, the Schrödinger equation cannot be solved analytically, and several approximations are needed to resolve the problem. Because of the large difference in mass, the heavy nuclei have much smaller velocities than the electrons, which rapidly adapt themselves to the nuclear motion. The electrons essentially perceive the nuclei as frozen in space, which allows the Schrödinger equation to be separated into distinct parts describing the electronic and nuclear wave functions. This separation,

*In atomic units, which are used throughout this thesis, the elementary charge e, electron mass m_e, reduced Planck's constant $\hbar$, and Coulomb's constant $1/(4\pi\epsilon_0)$ are all unity by definition.

known as the Born–Oppenheimer approximation,[46] reduces the problem to solving the electronic Schrödinger equation

$$\hat{H}_{\mathrm{el}}\psi_{\mathrm{el}} = (\hat{T}_{\mathrm{e}} + \hat{V}_{\mathrm{e,e}} + \hat{V}_{\mathrm{N,N}} + \hat{V}_{\mathrm{N,e}})\psi_{\mathrm{el}} = E_{\mathrm{el}}\psi_{\mathrm{el}} \tag{2.4}$$

for a fixed set of nuclear geometries. The electronic wave function ψ_{el} has only a parametric dependence on the positions of the nuclei, but is independent of their momenta. Furthermore, since the nuclear–nuclear repulsion term $\hat{V}_{\mathrm{N,N}}$ is constant for frozen nuclei, it only shifts the eigenvalues, but does not otherwise affect the solution of the electronic Schrödinger equation.

Even with the Born–Oppenheimer approximation, the Schrödinger equation remains difficult to solve accurately, since the exact wave function is unknown. However, the task is facilitated by the variational principle[47,48]

$$\langle E \rangle = \frac{\langle \Phi | \, \hat{H} \, | \Phi \rangle}{\langle \Phi | \Phi \rangle} \geq E_0, \tag{2.5}$$

according to which the expectation value of the energy, $\langle E \rangle$, of *any* trial wave function Φ is an upper bound to the true ground state energy E_0. This allows the best wave function of a given form to be found by minimizing the energy with respect to the parameters of the trial function.

The variational principle also leads[49] to another property of the quantum system, known as the Hellmann–Feynman theorem,[50–52] which is especially useful in calculating intermolecular forces in molecules. This theorem, obeyed by all variational wave functions,[53] relates a variation of a parameterized Hamiltonian to a corresponding change in energy, according to

$$\frac{\mathrm{d}E_\lambda}{\mathrm{d}\lambda} = \left\langle \Psi_\lambda \middle| \frac{\mathrm{d}\hat{H}_\lambda}{\mathrm{d}\lambda} \middle| \Psi_\lambda \right\rangle, \tag{2.6}$$

where the energy E_λ, the normalized wave function Ψ_λ, and the Hamiltonian $\hat{H}_\lambda$ all depend on the continuous parameter λ.

2.2 Hartree–Fock Method

The Coulombic repulsion of the electrons is one of the main reasons why the electronic Schrödinger equation is so difficult to solve, since it prevents the Hamiltonian from being separable into distinct components for each electron. One of the simplest techniques developed to overcome this obstacle is the Hartree–Fock (HF) method, in which the electron repulsion term is replaced by a mean field so that a given electron only feels the average effect of its neighbors. This procedure enables the N-electron Schrödinger equation to be recast as N coupled one-electron equations, whose solutions are used to approximately represent the electronic wave function ψ_{el} as a Slater determinant[54,55]

$$\Phi_{\mathrm{HF}}(\mathbf{x}_1, \mathbf{x}_2, \ldots, \mathbf{x}_N) = \frac{1}{\sqrt{N!}} \begin{vmatrix} \phi_1(\mathbf{x}_1) & \phi_2(\mathbf{x}_1) & \cdots & \phi_N(\mathbf{x}_1) \\ \phi_1(\mathbf{x}_2) & \phi_2(\mathbf{x}_2) & \cdots & \phi_N(\mathbf{x}_2) \\ \vdots & \vdots & \ddots & \vdots \\ \phi_1(\mathbf{x}_N) & \phi_2(\mathbf{x}_N) & \cdots & \phi_N(\mathbf{x}_N) \end{vmatrix}, \tag{2.7}$$

where the functions ϕ_i are one-electron spin orbitals, and $\mathbf{x}_k$ denotes the spin and spatial degrees of freedom of electron k. This representation fulfills the antisymmetry requirement

$$\psi_{\mathrm{el}}(\ldots, \mathbf{x}_i, \ldots, \mathbf{x}_j, \ldots) = -\psi_{\mathrm{el}}(\ldots, \mathbf{x}_j, \ldots, \mathbf{x}_i, \ldots), \tag{2.8}$$

which states that since electrons are indistinguishable fermions, the wave function must change sign if any two electron coordinates are interchanged.

With the restriction that the spin orbitals remain orthonormal, the variational minimization of the energy of a single Slater determinant leads to the Hartree–Fock equations

$$\hat{F}\phi_i = \epsilon_i \phi_i \tag{2.9}$$

for the spin orbitals ϕ_i and the orbital energies ϵ_i. The Fock operator $\hat{F}$ describes the kinetic energy of an electron together with the attraction to all the nuclei and the average repulsion to all other electrons.[53] Because this operator depends on all the occupied orbitals, it couples the HF equations requiring them to be solved iteratively. This process, known as the self-consistent field (SCF) method, begins with an initial guess for the spin orbitals. The new orbitals, which in turn serve as an initial guess for the next round of iterations, are calculated based on eq. (2.9), and the procedure is repeated until convergence. The number of optimized spin orbitals is usually greater than the number of electrons in the system, in which case only the orbitals with the lowest energies are occupied, i.e., used to construct the Slater determinant while the rest, the virtual orbitals, remain unoccupied.

The main source of error in the HF method is that it does not treat the electrons as discrete point particles, as a result of which the electronic energy of the system is in reality lower than that given by HF theory. The difference between the energies, known as the correlation energy, is mostly due to the fact that the mean field approximation allows the electrons to get too close to each other on average, leading to an overestimation of the Coulombic repulsion between the particles.[56] Even though the Fermi correlation—the tendency of electrons with parallel spins to avoid each other due to the antisymmetry principle—is included in the HF theory, the missing Coulomb correlation renders it too inaccurate for many chemical applications. This shortcoming has lead to the development of more advanced methods, which are better capable of describing the physical nature of the electrons.

2.3 Electron Correlation Methods

Many schemes developed to calculate the correlation energy are based on the premise that allowing electronic excitations to the virtual orbitals can improve the wave function and hence the energy. This is due to the fact that the wave function ψ_{el} of the system can be expanded as a linear combination of Slater determinants:

$$\psi_{\text{el}} = a_0 \Phi_{\text{ref}} + \sum_{i=1} a_i \Phi_i, \tag{2.10}$$

where Φ_{ref} is a reference state, which is used to construct the excited determinants Φ_i by replacing one or more of the occupied orbitals with virtual ones. The reference state is normally taken to be the Hartree–Fock determinant Φ_{HF}, since it usually accounts for about 99 % of the correct answer.[57] If the representation in eq. (2.10) includes all possible determinants that can be formed in a given one-electron basis, it is an exact solution to the electronic Schrödinger equation in that basis. Such an approach is taken in the full configuration interaction method (FCI), which hence recovers all of the correlation energy, but is impossible for all but the smallest systems due to the extreme computational resources required.

The simplest way to make the electron correlation problem tractable is to truncate the series in eq. (2.10) and ignore all high-order excitations, which contribute little

to the wave function. This method is known as configuration interaction (CI), but it is unfortunately not well suited to the study of intermolecular interactions, since ignoring some of the high-order excitations renders it impossible to calculate the energies of systems of differing sizes with the same accuracy. This problem is solved by the more accurate coupled cluster (CC) approach where an exponential wave function ansatz

$$\Phi_{\mathrm{CC}} = e^{\hat{T}}\Phi_{\mathrm{ref}} = \sum_{k=0}^{\infty} \frac{\hat{T}^k}{k!}\Phi_{\mathrm{ref}} \tag{2.11}$$

is used. The operator

$$\hat{T} = \sum_{i=1}^{n} \hat{T}_i \tag{2.12}$$

is a sum of excitation operators $\hat{T}_i$, which produce all excitations of order i from the reference state. This method has several variants, which are named based on the orders of the excitation operators retained in eq. (2.12). One of the simplest practical variants is the coupled cluster singles and doubles (CCSD) method, where excitations up to second order are included. Because of the Brillouin theorem,[58] the singly excited determinants alone do not improve the energy, although they are usually included in the CC ansatz since their number is relatively small, and they can indirectly affect the energy through coupling with other determinants.[53] A drawback of the coupled cluster method is that its standard formulation is not variational.[56] Furthermore, it is computationally demanding, and the triply excited determinants are often already too expensive to be rigorously included.

Besides an explicit determinant expansion such as that in eq. (2.10), the effects of electron correlation can be included by means of perturbation theory.[53,56,59] The idea is that a complicated system can often be treated as a perturbed version of a simpler idealized model, whose solutions are known. Mathematically, the Hamiltonian H is split as

$$H = H_0 + \lambda H', \tag{2.13}$$

where H_0 is the Hamiltonian for the simple system, and H' represents a perturbation, whose strength is indicated by the parameter λ. If the perturbation is small enough, the solutions to the full problem can be expressed as corrections to those of the reduced system by means of a power series in λ.

One of the most common methods based on perturbation theory is the Møller–Plesset (MP) theory,[60] in which H_0 is taken to be the sum of the one-electron Fock operators, whereas H' contains all other correlation effects. This approach introduces a hierarchy of methods called MPn, where n signifies the order upto which the perturbations are included. Since MP1 only recovers the Hartree–Fock energy E_{HF}, the lowest MP level of practical use is MP2, which essentially models the effects of double electronic excitations.[53] The corresponding energy can be expressed as[53]

$$E_{\mathrm{MP2}} = E_{\mathrm{HF}} + \sum_{i<j}^{\mathrm{occ}} \sum_{a<b}^{\mathrm{vir}} \frac{\langle \phi_i \phi_j || \phi_a \phi_b \rangle^2}{\epsilon_i + \epsilon_j - \epsilon_a - \epsilon_b}, \tag{2.14}$$

where ϕ_α is a spin-orbital with an energy ϵ_α, and the term in the brackets represents an antisymmetrized electron repulsion integral in the so-called physicist's notation (see pp. 95–96 of ref. 53). Møller–Plesset calculations beyond the second level are less common due to the uncertain convergence of the perturbation expansion, and in particular since the higher-order corrections are often characterized by a less favorable cost–accuracy ratio.[59]

Perturbation theory can also be used in conjunction with other methods in order to improve accuracy at a reduced computational cost. Most electronic structure calculations in this thesis have utilized the CCSD(T) method, where the effect of the triple excitations is approximately included via perturbation theory.

2.4 Basis Sets

For many-electron systems, the exact form of the molecular orbitals is unknown, although in some simple cases they can be represented numerically. However, in order to efficiently represent the electron distribution in a molecule, the molecular orbitals need to be expressed in terms of simple analytic functions. A method known as linear combination of atomic orbitals (LCAO) is frequently used to represent the molecular orbitals ϕ_i as

$$\phi_i = \sum_\alpha c_{i\alpha}\varphi_\alpha, \tag{2.15}$$

where each φ_α is an atomic orbital composed of one or more basis functions, which together constitute a basis set.

The angular part of all one-electron basis functions can be described by spherical harmonic functions, since they are an exact angular solution for a one-electron system in any central potential.[59,61] In a Slater-type orbital (STO), the radial part has the form[59]

$$R_{l\zeta}^{\mathrm{STO}}(r) = A_{l\zeta} r^l e^{-\zeta r}, \tag{2.16}$$

where $A_{l\zeta}$ is a constant depending on the parameters l and ζ. Although reminiscent of the solutions of the hydrogen-like one-electron problem, this functional form is challenging due to the excessive computational cost of the entailing molecular integrals. By expanding the basis functions in terms of Gaussian primitives

$$R_{l\alpha}^{\mathrm{GTO}}(r) \propto r^l e^{-\alpha r^2}, \tag{2.17}$$

the integral evaluation can be hastened even though more functions are needed in order to reach the same accuracy.[59]

The basis sets used in this thesis are predominantly of the valence triple-zeta quality, meaning that each valence atomic orbital is composed of three basis functions. Additionally, polarization and diffuse functions were used in order to increase accuracy and flexibility. The polarization functions have higher angular momenta than the occupied atomic orbitals, enabling them to better describe the anisotropic electron distribution due to bonding. The slowly decaying diffuse functions can capture long-range interactions, and are thus crucial for their proper description.

For heavy elements, the number of basis functions required to rigorously treat all electrons can significantly hinder the calculations. Increasing atomic numbers also engender more prominent relativistic effects due to their polynomial scaling with respect to the nuclear charge.[62,63] However, it is often unnecessary to treat the core electrons explicitly, since they typically remain relatively inactive in chemical interactions. Significant computational speedups can therefore be gained, if the inert core is modeled by a suitable pseudopotential, which can also be fitted to include scalar relativistic effects.[64,65] In the present study, this approach of relativistic pseudopotentials was utilized for all metal atoms.

Chapter 3

Intermolecular Interactions

Long-range forces are characterized by an inverse polynomial dependence on the intermolecular distance, as opposed to the much faster exponential decay of the interactions due to wavefunction overlap. The precise range of separations covered by these forces varies with the system: the intermolecular distance should be sufficiently large to disregard the antisymmetrization of the total wavefunction, but small enough to ignore the retardation effects[66] due to the finite speed of light.

Based on their physical origin, the long-range interactions can be divided into electrostatic, induction, and dispersion forces. The former two can be described by classical mechanics, where as the latter requires quantum-theoretical considerations. This thesis is centered on the efficient computational modeling of dispersion interactions, even though it is necessary to account for the other long-range forces as parts of the total interaction energy.

3.1 Coulombic Interactions

As atoms and molecules are partly composed of charged particles—the electrons and protons—they can interact with each other via the associated Coulombic forces. In a pair of interacting molecules, the charge cloud around each monomer reciprocally feels the effect of the other one, which leads to an interaction between them. This also alters the molecular charge distributions of the monomers, which in turn leads to higher-order interactions. The end result is a host of intricately coupled forces, which are ultimately responsible for all long-range intermolecular interactions between molecules.

In the following mathematical treatment, the Einstein summation convention is adopted for repeated Greek indices, which are used as placeholders to indicate the Cartesian coordinates x, y, or z. In this notation, the summation over all possible values is implied for the repeated index values. For example, a dot product in the Cartesian coordinates could be represented as $\mathbf{a} \cdot \mathbf{b} = a_\alpha b_\alpha \equiv a_x b_x + a_y b_y + a_z b_z$, where the latter terms are the Cartesian components of the vectors $\mathbf{a}$ and $\mathbf{b}$.

Potential Produced by a Molecule

Consider a localized charge distribution composed of discrete point charges, which is nonvanishing only inside a sphere of a given radius s. According to classical electrodynamics, the associated electric potential $V(\mathbf{R})$, at some point $\mathbf{R}$ outside the sphere, can be expanded in powers of $1/R$. The potential produced by a collection

of point charges, e_i, at the locations $\mathbf{r}_i$ is[67]

$$\begin{aligned} V(\mathbf{R}) &= \sum_i \frac{e_i}{|\mathbf{R}-\mathbf{r}_i|} = \sum_i e_i \sum_{n=0}^{\infty} \frac{(\mathbf{r}_i\cdot\nabla)^n}{n!} \frac{1}{|\mathbf{R}-\mathbf{r}_i|}\bigg|_{\mathbf{r}_i=0} \\ &= \sum_i e_i \left(\frac{1}{R} - r_{i\alpha}\nabla_\alpha \frac{1}{R} + \frac{1}{2} r_{i\alpha} r_{i\beta} \nabla_{\alpha\beta} \frac{1}{R} - \cdots \right), \end{aligned} \tag{3.1}$$

where $R = |\mathbf{R}|$, $r_{i\alpha}$ stands for a Cartesian component of the vector $\mathbf{r}_i$, and ∇ is the differential operator.

It is common to write eq. (3.1) in terms of traceless tensors, as the trace does not contribute to the overall potential, since the Coulomb kernel satisfies the Laplace equation. For example, the tensor $r_{i\alpha}r_{i\beta}$ can be replaced with the traceless quantity $M_{\alpha\beta} = r_{i\alpha}r_{i\beta} - r_i^2\delta_{\alpha\beta}/3$ without altering the potential, because $\delta_{\alpha\beta}\nabla_{\alpha\beta}R^{-1} = 0$. In general, the rank n traceless tensors $M^{(n)}_{\alpha\beta\ldots\nu}$ can be constructed from the solid spherical harmonic functions of degree n, and written as[68]

$$M^{(n)}_{\alpha\beta\ldots\nu} = \frac{(-1)^n}{(2n-1)!!} r_i^{2n+1} \nabla_{\alpha\beta\ldots\nu} \frac{1}{r_i}, \tag{3.2}$$

where $r_i = |\mathbf{r}_i|$. By inserting eq. (3.2) into eq. (3.1), the potential can be expressed as

$$V(\mathbf{R}) = \sum_{n=0}^{\infty} \frac{(-1)^n}{(2n-1)!!} T^{(n)}_{\alpha\beta\ldots\nu} \xi^{(n)}_{\alpha\beta\ldots\nu}, \tag{3.3}$$

where the rank n tensors

$$\xi^{(n)}_{\alpha\beta\ldots\nu} = \frac{(-1)^n}{n!} \sum_i e_i r_i^{2n+1} \nabla_{\alpha\beta\ldots\nu} \frac{1}{r_i} \tag{3.4}$$

$$T^{(n)}_{\alpha\beta\ldots\nu} = \nabla_{\alpha\beta\ldots\nu} \frac{1}{R} \tag{3.5}$$

are known as the multipole moment and the interaction tensor, respectively. Due to the Laplace equation and the invariance with respect to the order of the derivatives, they are totally symmetric and traceless with respect to contraction of any two indices. Instead of the ξ-notation, the low-order multipole moments are usually referred to by their common names and symbols. The moments with $n = 1-4$ are called the dipole, quadrupole, octupole, and hexadecapole, and possess the associated symbols μ, Θ, Ω, and Φ, respectively.

Even though the molecular charge distributions formally extend to infinity, the expansion can still be performed for them under certain conditions. The electronic wave function is usually expanded in terms of Gaussian orbitals, and in such a case the expansion is well defined as long as the radius s is large enough to include all the centers of the orbitals, which are usually located at the nuclei.[69]

Molecule in an External Potential

The energy of a molecule in a general non-uniform external potential $\phi(\mathbf{r})$ is described by the operator[70]

$$\mathcal{H}' = \sum_i e_i \hat{\phi}(\mathbf{r}_i), \tag{3.6}$$

where the summation runs over all the electrons and nuclei, with charges e_i located at points $\mathbf{r}_i$. Similar to eq. (3.1), the Taylor expansion of this potential is

$$\phi(\mathbf{r}) = \phi(0) + \phi_\alpha(0) r_\alpha + \frac{1}{2}\phi_{\alpha\beta}(0) r_\alpha r_\beta + \cdots , \tag{3.7}$$

where

$$\phi_{\alpha\beta\ldots\nu}(0) \equiv \frac{\partial^n}{\partial r_\alpha \partial r_\beta \cdots \partial r_\nu} \phi(\mathbf{r})\bigg|_{\mathbf{r}=0} \tag{3.8}$$

For potentials of molecular origin, eq. (3.7) can be written in terms of traceless multipole moment tensors as

$$\phi(\mathbf{r}) = \sum_{n=0}^{\infty} \frac{1}{(2n-1)!!} \xi^{(n)}_{\alpha\beta\ldots\nu} \phi_{\alpha\beta\ldots\nu}(0) \tag{3.9}$$

Interaction Potential

The Coulombic interaction between molecules can be calculated based on eqs. (3.3) and (3.9). Consider a unit charge at the point $\mathbf{r}_a$ relative to molecule A, centered at the location $\mathbf{A}$, and an analogous point charge relative to molecule B. The corresponding interaction potential is

$$V^{AB}(\mathbf{R}) = \frac{1}{|(\mathbf{B}+\mathbf{r}_b) - (\mathbf{A}+\mathbf{r}_a)|} = \frac{1}{|\mathbf{R} - \mathbf{r}_a + \mathbf{r}_b|}, \tag{3.10}$$

where $\mathbf{R} = \mathbf{B} - \mathbf{A}$. The generalization to several point charges is obtained by a trivial summation over the charges. If the derivative notation analogous to eq. (3.8) is adopted for $V^{AB}(\mathbf{R})$, the Taylor expansion with respect to molecule B, i.e., around the point $\mathbf{r}_b = 0$ is

$$V^{AB}(\mathbf{R}) = \sum_{n_B=0}^{\infty} \frac{1}{(2n_B-1)!!} \xi^{B(n_B)}_{\sigma\tau\ldots\omega} V^{AB}_{\sigma\tau\ldots\omega}(\mathbf{R})\bigg|_{\mathbf{r}_b=0} \tag{3.11}$$

where the derivatives are taken with respect to the components of $\mathbf{r}_b$, and $\xi^{B(n_B)}_{\sigma\tau\ldots\omega}$ signifies the rank n_B multipole moment of molecule B. Since

$$\frac{\partial^{n_B}}{\partial r_{b_\sigma} \partial r_{b_\tau} \cdots \partial r_{b_\omega}} V^{AB}(\mathbf{R})\bigg|_{\mathbf{r}_b=0} = \frac{\partial^{n_B}}{\partial R_\sigma \partial R_\tau \cdots \partial R_\omega} V^{AB}(\mathbf{R})\bigg|_{\mathbf{r}_b=0} \tag{3.12}$$

the expansion in eq. (3.11) can also be written as

$$V^{AB}(\mathbf{R}) = \sum_{n_B=0}^{\infty} \frac{1}{(2n_B-1)!!} \xi^{B(n_B)}_{\sigma\tau\ldots\omega} \nabla_{\sigma\tau\ldots\omega} \frac{1}{|\mathbf{R} - \mathbf{r}_a|}, \tag{3.13}$$

where the derivatives are now taken with respect to the components of $\mathbf{R}$. After inserting the expansion in eq. (3.3), the potential becomes

$$V^{AB}(\mathbf{R}) = \sum_{n_A=0}^{\infty} \sum_{n_B=0}^{\infty} \frac{(-1)^{n_A}}{(2n_A-1)!!} \frac{1}{(2n_B-1)!!} \xi^{A(n_A)}_{\alpha\beta\ldots\nu} T^{AB(n_A+n_B)}_{\alpha\beta\ldots\nu\sigma\tau\ldots\omega} \xi^{B(n_B)}_{\sigma\tau\ldots\omega}, \tag{3.14}$$

where the interaction potential is now expressed in terms of local multipoles of the molecules, coupled together by the rank $n_A + n_B$ interaction tensor $T^{AB(n_A+n_B)}_{\alpha\beta\ldots\nu\sigma\tau\ldots\omega}$.

Spherical Representation

The Cartesian representation of the Coulombic interactions is straightforward, but it has some drawbacks. For example, the rank n interaction tensor and multipole moments have 3^n Cartesian components, but not all of them are independent due to the symmetry and tracelessness requirements.[70,71] Furthermore, the Cartesian tensors are not ideally suited to the description of multipole moments, which are essentially harmonic homogeneous polynomials, as is reflected by their close relationship to the spherical harmonic functions.[70,72]

It would be advantageous to formulate the potential expansion in terms of harmonic functions, as they can more closely reflect the essence of the tensors at hand. For example, consider the number of independent tensor components. The dimension of the space of homogeneous harmonic polynomials of degree n in N variables is[73]

$$\dim \mathbf{H}_n(\mathbb{R}^N) = \binom{N+n-1}{N-1} - \binom{N+n-3}{N-1}, \tag{3.15}$$

which is also the number of independent components in a totally symmetric traceless tensor of rank n, as can be ascertained by a simple counting argument. Since a totally symmetric tensor is invariant with respect to permutations of the indices, the only factor that distinguishes between different components is the total amounts of the various indices. For example, the components T_{xxy}, T_{xyx}, and T_{yxx} are not all independent: since their index sets are composed of two x's and one y, the equality $T_{xxy} = T_{xyx} = T_{yxx}$ holds. As the amount of indices is equal to the rank, the number of independent components in a totally symmetric rank n tensor in N dimensions is the same as the number of N-tuples of non-negative integers, whose sum is n. According to an elementary theory in combinatorics,[74] this number is given by the binomial coefficient $\binom{N+n-1}{N-1}$. The number is further reduced by the tracelessness requirement, i.e., that the contraction of any two indices vanishes. By the same argument as before, the remaining $n-2$ indices lead to $\binom{N+(n-2)-1}{N-1}$ additional restraints. The difference of these two binomial coefficients thus gives the number of totally symmetric traceless rank n tensors in N dimensions, which amounts to $2n+1$ in the three dimensional space.

The spherical expansion of the interaction potential can be performed by replacing the Taylor series by an expansion given by the spherical harmonic addition theorem.[75] For the potential in eq. (3.10) this expansion takes the form[70]

$$V^{AB}(\mathbf{R}) = \sum_{l=0}^{\infty} \sum_{m=-l}^{l} (-1)^m R_{l,-m}(\mathbf{r}_a - \mathbf{r}_b) I_{l,m}(\mathbf{R}), \tag{3.16}$$

as long as $|\mathbf{R}| > |\mathbf{r}_a - \mathbf{r}_b|$. The functions $R_{l,m}$ and $I_{l,m}$ are respectively known as the regular and irregular solid harmonics, and in spherical coordinates they can be expressed in terms of the spherical harmonic functions $Y_l^{(m)}(\theta, \varphi)$ as

$$R_{l,m}(r, \theta, \varphi) = \sqrt{\frac{4\pi}{2l+1}} r^l Y_l^{(m)}(\theta, \varphi) \tag{3.17}$$

$$I_{l,m}(r, \theta, \varphi) = \sqrt{\frac{4\pi}{2l+1}} r^{-l-1} Y_l^{(m)}(\theta, \varphi). \tag{3.18}$$

An addition theorem for the solid harmonics[70,76] can be used to further expand the

term $R_{l,-m}(\mathbf{r}_a - \mathbf{r}_b)$, which results in

$$V^{AB}(\mathbf{R}) = \sum_{\substack{l_1,l_2 \\ m_1,m_2,M}} (-1)^{l_1} \sqrt{\frac{(2L+1)!}{(2l_1)!(2l_2)!}} \begin{pmatrix} l_1 & l_2 & L \\ m_1 & m_2 & M \end{pmatrix} \xi^A_{l_1,m_1} \xi^B_{l_2,m_2} I_{L,M}(\mathbf{R}), \quad (3.19)$$

where $L = l_1 + l_2$, and $\left(\begin{smallmatrix} l_1 & l_2 & L \\ m_1 & m_2 & M \end{smallmatrix}\right)$ is a Wigner 3-j symbol.[76] For the molecule A, composed of point charges e_a at locations $\mathbf{r}_a$, the spherical multipole moments are defined as

$$\xi^A_{l,m} = \sum_{a \in A} e_a R_{l,m}(\mathbf{r}_a), \quad (3.20)$$

and analogously for molecule B.

The multipole moments characterized by the indices l and m in eq. (3.20) are complex if $m \neq 0$, due to the corresponding property of the solid harmonics. It is often more convenient to work with real functions obtained from linear combinations of the solid harmonic functions. By replacing m with a new label κ, which can take the values[70,77] $lc, \ldots, 1c, 0, 1s, \ldots, ls$, and introducing the functions

$$R_{l,kc} = \frac{1}{\sqrt{2}} \left[(-1)^k R_{l,k} + R_{l,-k} \right] \quad (3.21)$$

$$R_{l,ks} = \frac{1}{i\sqrt{2}} \left[(-1)^k R_{l,k} - R_{l,-k} \right], \quad (3.22)$$

where $0 \leq k \leq l$, the real spherical multipole moments can be calculated as

$$\xi^A_{l,\kappa} = \sum_{a \in A} e_a R_{l,\kappa}(\mathbf{r}_a). \quad (3.23)$$

Another inconvenience with the spherical representation presented thus far is that it is formulated in terms of the global coordinate system. The multipole moments are normally considered in the local frame, i.e., as molecule fixed. For example, in the local frame, the dipole moment of a molecule is the same regardless of how it is oriented in space. However, in the global coordinate system, the orientation of the vectors, and hence the multipole moments, change as the molecule rotates.

The effect of the rotations can be accounted for in different ways. One method is to use the Wigner rotation matrices to transform the multipole moments from the global to the local frame,[70] which, however, leads to rather complicated expressions in terms of multiple summations over the elements of said matrices. A simpler method[77] is based on including the rotations already in the formula describing the interaction potential. In the local frame the potential is

$$V^{AB}(\mathbf{R}) = \frac{1}{|\mathbf{R} - \hat{R}_A \mathbf{r}_a + \hat{R}_B \mathbf{r}_b|}, \quad (3.24)$$

where $\hat{R}_X = \hat{R}(\phi_X, \theta_X, \varphi_X)$ is a rotation matrix describing the orientation of the molecule X in terms of the Euler angles $(\phi_X, \theta_X, \varphi_X)$. A spherical expansion of this potential leads to[77]

$$V^{AB}(\mathbf{R}) = \sum_{l_1,l_2} \sum_{\kappa_1,\kappa_2} \frac{(-1)^{l_1}}{(2l_1-1)!!} \frac{1}{(2l_2-1)!!} \xi^A_{l_1,\kappa_1} T^{AB}_{l_1,\kappa_1,l_2,\kappa_2} \xi^B_{l_2,\kappa_2}, \quad (3.25)$$

where all quantities are expressed in terms of real functions in the local frames. The interaction tensor in the spherical basis is[77]

$$T^{AB}_{l_1,\kappa_1,l_2,\kappa_2} = R_{l_2,\kappa_2}(\hat{R}_B^{-1} \nabla_{\mathbf{R}}) R_{l_1,\kappa_1}(\hat{R}_A^{-1} \nabla_{\mathbf{R}}) \frac{1}{R}, \quad (3.26)$$

where the solid harmonic functions have the vector derivative operator $\nabla_{\mathbf{R}}$ as a part of their arguments.

Polarizabilities

The multipole moments describing the charge distribution of a molecule are not invariable, and can change due to an external potential such as that produced by another molecule. The external field and its gradients cause a distortion in the molecular electric charge distribution, which in turn induces additional multipole moments in the molecule. The total observed multipole moment of a given rank is thus a sum of the static moment and all the induced moments. The coefficients characterizing the induced moments are known as polarizabilities, and they describe how the molecular charge distribution is distorted, or polarized, in an external field.[78]

In terms of the multipole moments and polarizabilities, the energy E of a molecule in an external potential $V(\mathbf{r})$ can be written as a perturbation series[70,79]

$$\begin{aligned} E = E^{(0)} &+ \sum_{l_1\kappa_1} \xi_{l_1\kappa_1} V_{l_1\kappa_1} - \frac{1}{2!} \sum_{l_1\kappa_1 l_2\kappa_2} \alpha_{l_1\kappa_1,l_2\kappa_2} V_{l_1\kappa_1} V_{l_2\kappa_2} \\ &+ \frac{1}{3!} \sum_{l_1\kappa_1 l_2\kappa_2 l_3\kappa_3} \beta_{l_1\kappa_1,l_2\kappa_2,l_3\kappa_3} V_{l_1\kappa_1} V_{l_2\kappa_2} V_{l_3\kappa_3} - \cdots , \end{aligned} \tag{3.27}$$

where $E^{(0)}$ is the energy of the free molecule, and the spherical derivatives of the potential are defined in terms of the solid harmonic function $R_{l\kappa}$ as $V_{l\kappa} = [(2l-1)!!]^{-1} R_{l\kappa}(\nabla) V(\mathbf{r})|_{\mathbf{r}=0}$. The regular multipole–multipole polarizability $\alpha_{l_1\kappa_1,l_2\kappa_2}$ describes the linear response of the molecule to the external field, while the higher order terms, known as hyperpolarizabilities, account for the nonlinear effects.[70,78,80] The polarizability also describes the multipole moments $\xi_{l_1\kappa_1}$ induced by the field $V_{l_2\kappa_2}$ as[70]

$$\frac{\partial E}{\partial V_{l_1\kappa_1}} = \xi_{l_1\kappa_1} - \sum_{l_2\kappa_2} \alpha_{l_1\kappa_1,l_2\kappa_2} V_{l_2\kappa_2} + \cdots , \tag{3.28}$$

where the static value $\xi_{l_1\kappa_1}$ is recovered at the limit of vanishing external potential. The polarizability tensors are totally symmetric, meaning that $\alpha_{l_1\kappa_1,l_2\kappa_2}$ also characterizes the multipole moment $\xi_{l_2\kappa_2}$ induced by the field $V_{l_1\kappa_1}$. For example, the dipole–quadrupole polarizability $\alpha_{1\kappa_1,2\kappa_2}$ describes the quadrupole moment induced by the electric field $V_{1\kappa_1}$ as well as the dipole moment induced by the field gradient $V_{2\kappa_2}$.

The effects of polarizable molecular electric charge distributions appear in the second order of the perturbation expansion in eq. (3.27), and standard second order perturbation theory can be used to express the multipole–multipole polarizability as[70]

$$\alpha_{l_1\kappa_1,l_2\kappa_2} = \sum_{m\neq 0} \frac{\langle 0|\, \hat{\xi}_{l_1\kappa_1} \,|m\rangle \langle m|\, \hat{\xi}_{l_2\kappa_2} \,|0\rangle + \langle 0|\, \hat{\xi}_{l_2\kappa_2} \,|m\rangle \langle m|\, \hat{\xi}_{l_1\kappa_1} \,|0\rangle}{E_m - E_0}. \tag{3.29}$$

The lowest-order polarizability tensor is the dipole–dipole polarizability, since the charge terms ($l_1 = 0$ or $l_2 = 0$) are scalars, whose matrix elements vanish between orthogonal states. In Cartesian coordinates, the dipole–dipole polarizability can be written as

$$\alpha_{\alpha\beta} = \sum_{m\neq 0} \frac{\langle 0|\, \hat{\mu}_\alpha \,|m\rangle \langle m|\, \hat{\mu}_\beta \,|0\rangle + \langle 0|\, \hat{\mu}_\beta \,|m\rangle \langle m|\, \hat{\mu}_\alpha \,|0\rangle}{E_m - E_0}, \tag{3.30}$$

and an analogous definition in terms of the Cartesian multipole moments is also possible for the higher-order terms, although the Cartesian formulas are usually defined[81] with an additional factor of $[(2l-1)!!]^{-1}$ when $l_1 = l_2 = l$.

If the external electric field is not static but periodic, and oscillates with an angular frequency ω, time-dependent perturbation theory must be used to describe the interaction of a molecule with the field.[80] The effect of the oscillating field is that the polarizabilities become dynamic, i.e., dependent on the frequency ω. The dynamic dipole–dipole polarizability is[80]

$$\alpha_{\alpha\beta}(\omega) = \sum_{m\neq 0} \frac{\varepsilon_m \left(\langle 0| \hat{\mu}_\alpha |m\rangle \langle m| \hat{\mu}_\beta |0\rangle + \langle 0| \hat{\mu}_\beta |m\rangle \langle m| \hat{\mu}_\alpha |0\rangle \right)}{\varepsilon_m^2 - \omega^2}, \tag{3.31}$$

where $\varepsilon_m = E_m - E_0$. Formulas analogous to eq. (3.31) can also be derived for the higher-order dynamic polarizabilities, and the static formulas are recovered when $\omega = 0$.[80]

3.2 Perturbative Multipole Expansion

At long distances, intermolecular interactions represent a tiny fraction of the total energy of the system, which poses demands of accuracy and precision for the associated electronic structure calculation. The silver lining is that such a situation is well suited for a perturbative treatment, as the short-range electron exchange effects can be neglected for well separated molecules.[70] The only interaction thus results from the Coulombic forces between the particles of the monomers,[82] described by the perturbing Hamiltonian[70]

$$H' = \sum_{a\in A} \sum_{b\in B} \frac{e_a e_b}{r_{ab}}, \tag{3.32}$$

where the summations are over all particles (electrons and nuclei) of molecules A and B. The charges of the particles are indicated by e_a and e_b, and r_{ab} is the distance between them.

By expressing the potential in eq. (3.32) in terms of electric multipoles, the interaction can be described in terms of monomer properties. The perturbation becomes[83]

$$H' = \sum_{n_A, n_B} \frac{(-1)^{n_A}}{(2n_A-1)!!} \frac{1}{(2n_B-1)!!} \hat{\xi}^{A(n_A)}_{\alpha\beta\ldots\nu} T^{AB(n_A+n_B)}_{\alpha\beta\ldots\nu\sigma\tau\ldots\omega} \hat{\xi}^{B(n_B)}_{\sigma\tau\ldots\omega}, \tag{3.33}$$

where $\hat{\xi}^{A(n_A)}_{\alpha\beta\ldots\nu}$ is the rank n_A multipole moment operator for the molecule A. The Cartesian components of this operator are specified by the n_A subscripts $\alpha\beta\ldots\nu$, each of which can take the value of x, y or z. The tensor $T^{AB(n_A+n_B)}_{\alpha\beta\ldots\nu\sigma\tau\ldots\omega}$ describes dependence of the interaction on the orientations of the monomers. For molecules A and B, respectively centered at points $\mathbf{A}$ and $\mathbf{B}$, it is of the general form

$$T^{AB(n)}_{\alpha\beta\ldots\nu} = \nabla_\alpha \nabla_\beta \cdots \nabla_\nu \frac{1}{R}, \tag{3.34}$$

where $R = |\mathbf{B} - \mathbf{A}|$.

Polarization Approximation

The assumption of negligible electron exchange allows the electrons of the system to be assigned to the constituent molecules. For two interacting molecules A and

B, the unperturbed Hamiltonian H_0 is a sum of the individual Hamiltonians H_A and H_B, which describe the monomers in terms of their respective electrons. The unperturbed system can thus be described via the wavefunctions $\psi_m^A = |m\rangle$ and $\psi_n^B = |n\rangle$ as product states $|mn\rangle = |m\rangle\,|n\rangle$. With the perturbation given in eq. (3.33), Rayleigh–Schrödinger perturbation theory[84] can be used to derive the interaction energy E_{int}. In case of closed-shell molecules in a non-degenerate ground state $|00\rangle$ of the system, this results in the expansion

$$E_{\text{int}} = E - E_A - E_B = E^{(1)} + E^{(2)} + \cdots\,, \tag{3.35}$$

where E_A and E_B are the unperturbed energies of molecules A and B, and E is the total energy. In the context of intermolecular forces, eq. (3.35) is also referred to as the polarization approximation.[85,86]

The perturbative corrections can be expressed as[70]

$$E^{(1)} = \langle 00|\, H' \,|00\rangle \tag{3.36}$$

$$E^{(2)} = -\sum_{mn\neq 00} \frac{\langle 00|\, H' \,|mn\rangle\,\langle mn|\, H' \,|00\rangle}{(E_m - E_0) + (E_n - E_0)}, \tag{3.37}$$

where E_k is the energy associated with the state $|k\rangle$, and the summation is over states for which $m \neq 0 \vee n \neq 0$. Since the perturbation H' was of Coulombic origin, its expectation value, $E^{(1)}$, is equal to the electrostatic interaction energy E_{elst}. The second-order correction is composed of separate parts describing induction and dispersion:

$$E^{(2)} = E_{\text{ind}}^A + E_{\text{ind}}^B + E_{\text{disp}}, \tag{3.38}$$

where E_{ind}^A is the induction energy for molecule A, and E_{ind}^B is the analogous quantity for molecule B. Their sum-over-states expressions result from eq. (3.37) by setting $n = 0$ and $m = 0$, respectively. The dispersion energy is

$$E_{\text{disp}} = -\sum_{\substack{m\neq 0\\ n\neq 0}} \frac{\langle 00|\, H' \,|mn\rangle\,\langle mn|\, H' \,|00\rangle}{(E_m - E_0) + (E_n - E_0)}, \tag{3.39}$$

where the summation is restricted to states with $m \neq 0 \wedge n \neq 0$, signifying that both molecules A and B are excited.

High-Order Interactions

If the perturbation series is continued further, higher-order corrections to the induction and dispersion energies result.[87–92] The third-order energy can be represented as[91,93]

$$E^{(3)} = E_{\text{ind}}^{(3)} + E_{\text{disp}}^{(3)} + E_{\text{ind-disp}}^{(3)}, \tag{3.40}$$

where the first two terms on the right hand side represent contributions mainly due to the interaction of mutually polarized molecular charge clouds, along with nonlinear polarization effects.[88,91] The coupled induction-dispersion energy $E_{\text{ind-disp}}^{(3)}$ represents a modification to the dispersion interaction; it arises when the charge distribution of one molecule is distorted by the static field of the other.[88,91,92]

The multipole expansion can be continued to arbitrary orders, but in practice the physical significance of the higher order terms is often questionable. This is partly due to the fact that the perturbative multipole expansion does not necessarily converge,[94–100] and even in the third order a thorough description of the interactions

might require the inclusion of the terms due to electron exchange.[93] On the other hand, as the multipole expansion is essentially a power series in R^{-1}, the higher order terms have an increasingly steep distance dependence, signifying that they are only meaningful at small intermolecular distances. However, at such distances the underlying perturbative treatment ceases to apply, as the wave function overlap effects begin to dominate the interaction—it is therefore uncommon to apply the expansion to high orders.

Pairwise Additivity

Most long-range forces are not pairwise additive, but additional perturbative corrections emerge when more than two systems simultaneously interact with one another.[70,101,102] Only the electrostatic interactions are free of these many-body contributions, which affect the induction and dispersion energies to varying degrees. While the non-additivity effect in the dispersion energy is seldom significant, pair-potentials completely fail to describe the induction interactions. The reason for this failure is that the induction energy between two molecules is proportional to the total electric field, which can be drastically altered by the static fields of the surrounding molecules.

The second-order dispersion energy is strictly pairwise additive, but in the third order of perturbation theory, non-additive terms arise. The most important of these is the three-body Axilrod–Teller–Muto[103,104] (ATM) term

$$E_{\mathrm{ATM}} = C_9 \frac{1 + 3\cos\theta_1 \cos\theta_2 \cos\theta_3}{R_1^3 R_2^3 R_3^3}, \tag{3.41}$$

where C_9 is a positive constant, and R_i and θ_i are the side lengths and interior angles, respectively, of the triangle formed by three interacting species. It is noteworthy that the geometrical factor in eq. (3.41) permits both attractive and repulsive interactions, where as the second order dispersion energy is always strictly negative. The ATM term is sometimes referred to as the triple-dipole term, as it stems from the dipole terms of the multipole expansion. Higher-order multipoles produce additional terms[101,105–107] to the non-additive third-order energy, but they do not generally contribute significantly to the total intermolecular interaction energy at long distances.

3.3 Electrostatic Interaction

Out of all the long-range intermolecular interaction terms, the quantum-mechanical electrostatic and induction forces are perhaps the easiest to understand, since they correspond to their classical analogues, and quantum theory is only required to give an expression to the multipole moments and polarizabilities, which describe the strength of the interaction.[70]

The electrostatic energy, E_{elst}, is the lowest-order term in the polarization approximation, and it is caused by the interaction between the permanent charge clouds of the molecules. This interaction is present among most interacting species: only molecules with spherically symmetric charge distributions, such as rare gas atoms, do not experience the electrostatic force, because they have no electrical multipole moments. In principle, the electrostatic energy can be calculated directly from the definitions in eqs. (3.32) and (3.36). The downside is that such a procedure does not

yield a functional form of the electrostatic energy, and the calculation would thus have to be repeated if the geometry of the system changes.

Instead of the impractical direct approach, the multipole expansion can be used to obtain convenient approximations of the electrostatic term at large intermolecular distances. Usually only a few terms are required for an accurate approximation, and the required multipole moments and interaction functions can be calculated once and for all, and tabulated for later use. An explicit functional form of the interaction is recovered as well. However, this method is valid only for well separated molecules, although in some cases a distributed formulation of the multipoles can be used to circumnavigate this limitation.[108–110]

In the polarization approximation, the electrostatic energy can be calculated as the expectation value of the perturbing Hamiltonian H' with respect to the unperturbed states. In practice, this amounts to replacing the multipole moment operators in H' with their corresponding eigenvalues, i.e., the multipole moments themselves. In the Cartesian or spherical basis, the electrostatic interaction terms can thus be calculated from eqs. (3.14) and (3.25), respectively.

Symmetry and group theory can be used to determine the possible non-zero multipole moment components of a molecule, and thus simplify the treatment of the electrostatic interactions.[80,102,111,112] Most molecules studied in this thesis are linear or symmetric tops, and possess dihedral symmetry, meaning that they cannot have a dipole moment.[102] The lowest-order electrostatic interaction term between these molecules is thus the quadrupole–quadrupole interaction. A general quadrupole has five non-vanishing independent components, resulting in a sum of 25 terms for the quadrupole–quadrupole interaction. However, this number is greatly reduced in the case of symmetric tops, whose quadrupole moments can be described by a single component.[112] If the local z-axis is aligned with the highest-order rotation axis, this component is $\Theta \equiv \Theta_{zz}$ in the Cartesian basis, which equals the $\Theta_{2,0}$ component in the spherical basis.[70,111] The corresponding interaction energy in the spherical notation is

$$E_{\Theta\Theta} = \frac{1}{9}\Theta^A T^{AB}_{2,0,2,0}\Theta^B, \tag{3.42}$$

where the orientation dependence of the interaction is included in the tensor $T^{AB}_{2,0,2,0}$, which can be calculated from eq. (3.26), or looked up from tabulated values.[70,77] Based on this value, the explicit form of the interaction can be calculated from[70,101]

$$\begin{aligned} E_{\Theta\Theta} = \frac{3\Theta^A\Theta^B}{4R^5} \big[& 1 - 5\cos^2\theta_A - 5\cos^2\theta_B - 15\cos^2\theta_A\cos^2\theta_B \\ & + 2\left(4\cos\theta_A\cos\theta_B - \sin\theta_A\sin\theta_B\cos\varphi\right)^2 \big], \end{aligned} \tag{3.43}$$

where $R = |\mathbf{R}|$ is the distance between the centers of mass of the molecules. The angles specify the orientations of the molecules with respect to the vector $\mathbf{R}$, as depicted in fig. 4.1 on page 22.

Given the non-vanishing multipole moments of the molecules, a similar analysis can be used to derive all the other electrostatic interaction terms as well. The majority of the molecules studied in this thesis contain an inversion center, and can thus only possess multipoles of even rank.[112] The most important higher-order electrostatic terms for such systems are the quadrupole–hexadecapole and hexadecapole–hexadecapole interactions, with distance dependences of R^{-7} and R^{-9}, respectively. In general, the distance dependence for the electrostatic interaction between multipoles of ranks l_1 and l_2 is $R^{-l_1-l_2-1}$, because the corresponding T tensor is obtained by $l_1 + l_2$ fold differentiation of the function R^{-1}.

3.4 Induction Interaction

The electric potential of one molecule can cause the redistribution of the electric charge, i.e., electrostatic induction, in another molecule nearby. The induced multipole moments, which describe the extent of the redistribution, result in additional intermolecular interaction terms, separate from the electrostatic interactions caused by the static moments. These effects occur in the second order of the long-range perturbation theory, and are thus generally weaker than the electrostatic interactions. In the systems studied in this thesis, the induction contributions have been found insignificant, mostly due to the steep distance dependence (R^{-8} for the leading-order term) of the interactions, and the nonpolar nature of the molecules under inspection. In general, the leading-order induction energy of a molecule in an external potential V is[70,80,101]

$$E_{\text{ind}} = -\frac{1}{2} F_\alpha \alpha_{\alpha\beta} F_\beta + \cdots , \tag{3.44}$$

where $\alpha_{\alpha\beta}$ is the polarizability of the molecule, and F_α and F_β are the components of the electric field $F = -\nabla V$, evaluated at the center of mass of the molecule. The expansion in eq. (3.3) can be used to express the electric field produced by another molecule in terms of its static multipole moments, and the explicit formula for the energy can be derived from the intermolecular interaction tensor, as was the case for the electrostatic interactions. Stone and Tough have used the spherical tensor theory to derive an expression for the induction energy, applicable to arbitrary systems.[113]

3.5 Dispersion Interaction

The electrostatic and induction interactions result from the electromagnetic forces caused by *permanently* distorted molecular charge clouds. However, the electrons of all atoms and molecules are in constant motion, which produces transient oscillations in the electron density, leading to temporary fluctuating distortions in the charge clouds. The distortions in different molecules can interact with each other, resulting in an eventual synchronization of the oscillations and an attractive force between the molecules. The associated interaction energy is referred to as the dispersion energy, due to the connection to the physical mechanism responsible for the dispersion of light in a gas.[101]

The synchronization of coupled oscillators is common in classical physical and biological systems, and experienced, for example, by metronomes placed on a freely moving platform.[114] However, unlike for the electrostatic and induction energies, where quantum-mechanics was only required to give an expression for the multipole moments, no classical counterpart exists for the dispersion energy. A simple explanation for this was provided by London,[15] based on a model originally due to Drude.[115] In this model, an atom is represented by a nucleus and an electron cloud bound to it by a harmonic potential. If the charges of two interacting oscillators are artificially displaced from their rest positions, transient electric dipoles are formed, and the system becomes coupled through the dipole–dipole interaction. Classically, the two atoms in their equilibrium positions would not interact with each other, and the system would have a minimum energy of zero regardless of the coupling. However, a quantum-mechanical particle cannot lie absolutely at rest because of the zero-point motion due to Heisenberg's uncertainty principle.[116,117] The interaction between the transient dipoles is thus present in all atoms and molecules even if they do not possess permanent multipole moments. The resulting decrease of the total

energy, compared with the zero-point energies of the uncoupled atoms, turns out to be proportional to the second power of the strength of the coupling.[15,70,101] In the case of the dipole coupling, this strength vanishes as the inverse third power of the intermolecular distance R,[70] which leads to a dispersion energy contribution $E_{\text{disp}} \sim R^{-6}$.

The Drude model offers a straightforward explanation for the dispersion force, but it is only an approximation, since in reality the negative charge distribution around the interacting atoms is slightly distorted, producing a static polarization of the atoms towards each other. According to Feynman,[51] it is the attraction of each nucleus to its own distorted negative charge distribution, which is responsible for the van der Waals force, as opposed to interaction of the dipoles with each other.

A more satisfactory description can be obtained by means of perturbation theory. In the polarization approximation, the dispersion energy is given according to eq. (3.39) as a second order correction to the energy, and calculated via a sum over the excited states of the interacting molecules. In terms of the multipole expansion, the dispersion energy is obtained by replacing the interaction operator H' with its expanded form, i.e., either the Cartesian expression in eq. (3.33) or the spherical equivalent based on eq. (3.25). In fact, the expansion produces a range of terms, each proportional to some inverse power of the intermolecular distance. The lowest-order term in the dispersion interaction is produced by the dipole–dipole term, which can be expressed in Cartesian coordinates as[70,102]

$$\begin{aligned} E^{(6)}_{\text{disp}} &= -\sum_{\substack{m\neq 0\\ n\neq 0}} \frac{\langle 00|\, \hat{\mu}^A_\alpha T^{AB}_{\alpha\beta} \hat{\mu}^B_\beta \,|mn\rangle \,\langle mn|\, \hat{\mu}^A_\gamma T^{AB}_{\gamma\delta} \hat{\mu}^B_\delta \,|00\rangle}{(E_m - E_0) + (E_n - E_0)} \\ &= -T^{AB}_{\alpha\beta} T^{AB}_{\gamma\delta} \sum_{\substack{m\neq 0\\ n\neq 0}} \frac{\langle 0|\, \hat{\mu}^A_\alpha \,|m\rangle \,\langle m|\, \hat{\mu}^A_\gamma \,|0\rangle \,\langle 0|\, \hat{\mu}^B_\beta \,|n\rangle \,\langle n|\, \hat{\mu}^B_\delta \,|0\rangle}{(E_m - E_0) + (E_n - E_0)}. \end{aligned} \tag{3.45}$$

Even in charged molecules there are no dispersion terms corresponding to the total charge q, since it is a scalar, and its matrix elements between orthogonal eigenstates vanish.

The sum-over-states formula in eq. (3.45) is impractical, since it requires knowing the transition dipole moments to all discrete and continuum states.[102] A more convenient method is based on the work of Casimir and Polder,[66] and relies on the integral identity[70,101,102]

$$\frac{1}{a+b} = \frac{2}{\pi} \int_0^\infty \frac{ab}{(a^2+\omega^2)(b^2+\omega^2)}\, \mathrm{d}\omega, \tag{3.46}$$

valid for positive values of a and b. This formula allows eq. (3.45) to be written as

$$\begin{aligned} E^{(6)}_{\text{disp}} &= -\frac{2}{\pi} T^{AB}_{\alpha\beta} T^{AB}_{\gamma\delta} \int_0^\infty \sum_{m\neq 0} \frac{\varepsilon_m \,\langle 0|\, \hat{\mu}^A_\alpha \,|m\rangle \,\langle m|\, \hat{\mu}^A_\gamma \,|0\rangle}{\varepsilon_m^2 + \omega^2} \sum_{n\neq 0} \frac{\varepsilon_n \,\langle 0|\, \hat{\mu}^B_\beta \,|n\rangle \,\langle n|\, \hat{\mu}^B_\delta \,|0\rangle}{\varepsilon_n^2 + \omega^2}\, \mathrm{d}\omega \\ &= -\frac{1}{2\pi} T^{AB}_{\alpha\beta} T^{AB}_{\gamma\delta} \int_0^\infty \alpha^A_{\alpha\gamma}(i\omega) \alpha^B_{\beta\delta}(i\omega)\, \mathrm{d}\omega, \end{aligned} \tag{3.47}$$

where $\alpha^A_{\alpha\gamma}(i\omega)$ and $\alpha^B_{\beta\delta}(i\omega)$ are components of the polarizability tensor at an imaginary frequency, and $\varepsilon_m = E_m - E_0$. For spherically symmetric atoms, there is only one independent component,[80] $\bar{\alpha} = (\alpha_{xx} + \alpha_{yy} + \alpha_{zz})/3$, of the polarizability tensor, and

$\alpha_{\alpha\gamma}(i\omega) = \bar{\alpha}(i\omega)\delta_{\alpha\gamma}$. For such systems, the leading-order dispersion energy is thus reduced to[70,102]

$$\begin{aligned} E^{(6)}_{\text{disp}} &= -\frac{1}{2\pi} T^{AB}_{\alpha\beta} T^{AB}_{\alpha\beta} \int_0^\infty \bar{\alpha}^A(i\omega)\bar{\alpha}^B(i\omega)\,\mathrm{d}\omega \\ &= -\frac{1}{R^6}\frac{3}{\pi}\int_0^\infty \bar{\alpha}^A(i\omega)\bar{\alpha}^B(i\omega)\,\mathrm{d}\omega. \end{aligned} \tag{3.48}$$

The orientation dependence of the dispersion interaction is more complicated between linear molecules, as they have two independent polarizability components: one along the molecular axis, and another parallel to it, denoted $\alpha_\parallel$ and $\alpha_\perp$, respectively. The corresponding explicit form of the dispersion interaction can be written as[70]

$$\begin{aligned} E^{(6)}_{\text{disp}} = -\frac{C_6}{R^6}\Big\{1 &+ \frac{\gamma_{202}}{2}\left(3\cos^2\theta_1 - 1\right) + \frac{\gamma_{022}}{2}\left(3\cos^2\theta_2 - 1\right) \\ &+ \frac{\gamma_{22}}{2}\left[\left(2\cos\theta_1\cos\theta_2 - \sin\theta_1\sin\theta_2\cos\varphi\right)^2 - \cos^2\theta_1 - \cos^2\theta_2\right]\Big\}, \end{aligned} \tag{3.49}$$

where the angles describing the orientation of the system are defined as in fig. 4.1 on page 22. The dispersion coefficients are[70,113]

$$C_6 = \frac{3}{\pi}\int_0^\infty \bar{\alpha}^A(i\omega)\bar{\alpha}^B(i\omega)\,\mathrm{d}\omega \tag{3.50}$$

$$C_6\gamma_{202} = \frac{1}{\pi}\int_0^\infty \Delta\alpha^A(i\omega)\bar{\alpha}^B(i\omega)\,\mathrm{d}\omega \tag{3.51}$$

$$C_6\gamma_{022} = \frac{1}{\pi}\int_0^\infty \bar{\alpha}^A(i\omega)\Delta\alpha^B(i\omega)\,\mathrm{d}\omega \tag{3.52}$$

$$C_6\gamma_{22} = \frac{1}{\pi}\int_0^\infty \Delta\alpha^A(i\omega)\Delta\alpha^B(i\omega)\,\mathrm{d}\omega, \tag{3.53}$$

where $\bar{\alpha} = (\alpha_\parallel + 2\alpha_\perp)/3$, and $\Delta\alpha = \alpha_\parallel - \alpha_\perp$.

The higher-order dispersion interactions can be analyzed in a similar manner, in terms of the molecular polarizabilities. The spherical formulation allows the total dispersion energy to arbitrary order to be written as[70]

$$E_{\text{disp}} = -\frac{1}{2\pi}\sum_{\substack{l_1,l_2,l_3,l_4\\ \kappa_1,\kappa_2,\kappa_3,\kappa_4}} T^{AB}_{l_1\kappa_1,l_2\kappa_2} T^{AB}_{l_3\kappa_3,l_4\kappa_4}\int_0^\infty \alpha^A_{l_1\kappa_1,l_3\kappa_3}(i\omega)\alpha^B_{l_2\kappa_2,l_4\kappa_4}(i\omega)\,\mathrm{d}\omega, \tag{3.54}$$

where the orientation dependence is encompassed by the spherical T tensors.

Chapter 4

Results

The articles included in this thesis are centered around the computation and modeling of dispersion and other long-range interactions in coinage and volatile metal clusters. The total interaction energies of the model systems are calculated at long intermolecular distances, and divided into different physical contributions based on the polarization approximation. The electrostatic interactions are expressed in terms of the multipole expansion, and explicitly taken into account, while the induction interactions are found to be largely overshadowed by the leading order electrostatic and dispersion terms.

Articles I and II present a pair-potential approach to express the dispersion energy in terms of orientation-dependent interatomic van der Waals coefficients, which are calculated from small model systems. In Article III, the resulting coefficients are shown to accurately account for the dispersion energy in larger volatile metal clusters. Even the calculated isotropic dispersion coefficients manage to provide a faithful representation of the dispersion interactions, while the orientation dependent coefficients further improve the results. Theoretical aspects of the long-range interactions are explored in the final article. Concepts drawn from combinatorics and the geometric Clifford algebra are used to express the intermolecular interaction tensor in a novel form, which offers a simple and effective route to the formulas governing the long-range interactions in arbitrary systems. An implementation of the results along with some explicit examples are provided, and the formulation is applied to the calculation of intermolecular effects in systems composed of hydrogen and coinage metal clusters.

4.1 Studied Systems

The majority of the systems studied in this thesis are small dimer–dimer clusters composed of coinage and volatile metals. The geometry of the dimer systems is schematically represented in fig. 4.1. The global z-axis is aligned with the line connecting the centers of mass of the two dimers, distance R apart. The local z-axes of the dimers are aligned with the bond axes. For example, the $\Theta_{zz}^{\mathrm{Cu}}$ component of the quadrupole moment thus always refers to the component along the Cu–Cu bond, regardless of the orientation.

Besides the dimer clusters, some larger systems have been studied as well. In Article I, the silver–naphthalene system was used to calculate the silver–carbon dispersion coefficients. Three different clusters were used, of which one is depicted in fig. 4.2. The structures of the volatile metal clusters studied in Article III are presented in fig. 4.3. The orientation of the coordinate axes is similar to the dimer–

dimer clusters. For the nonlinear clusters, the local z-axis is oriented along the normal of molecular plane.

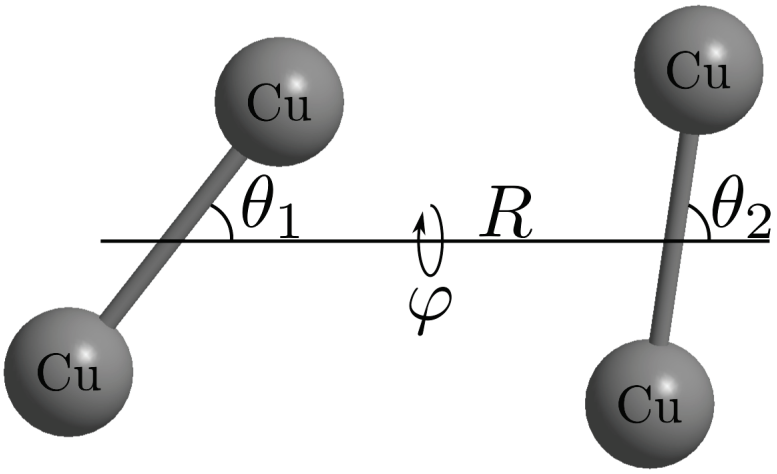

Figure 4.1: The coordinates describing the relative orientation of two dimers.

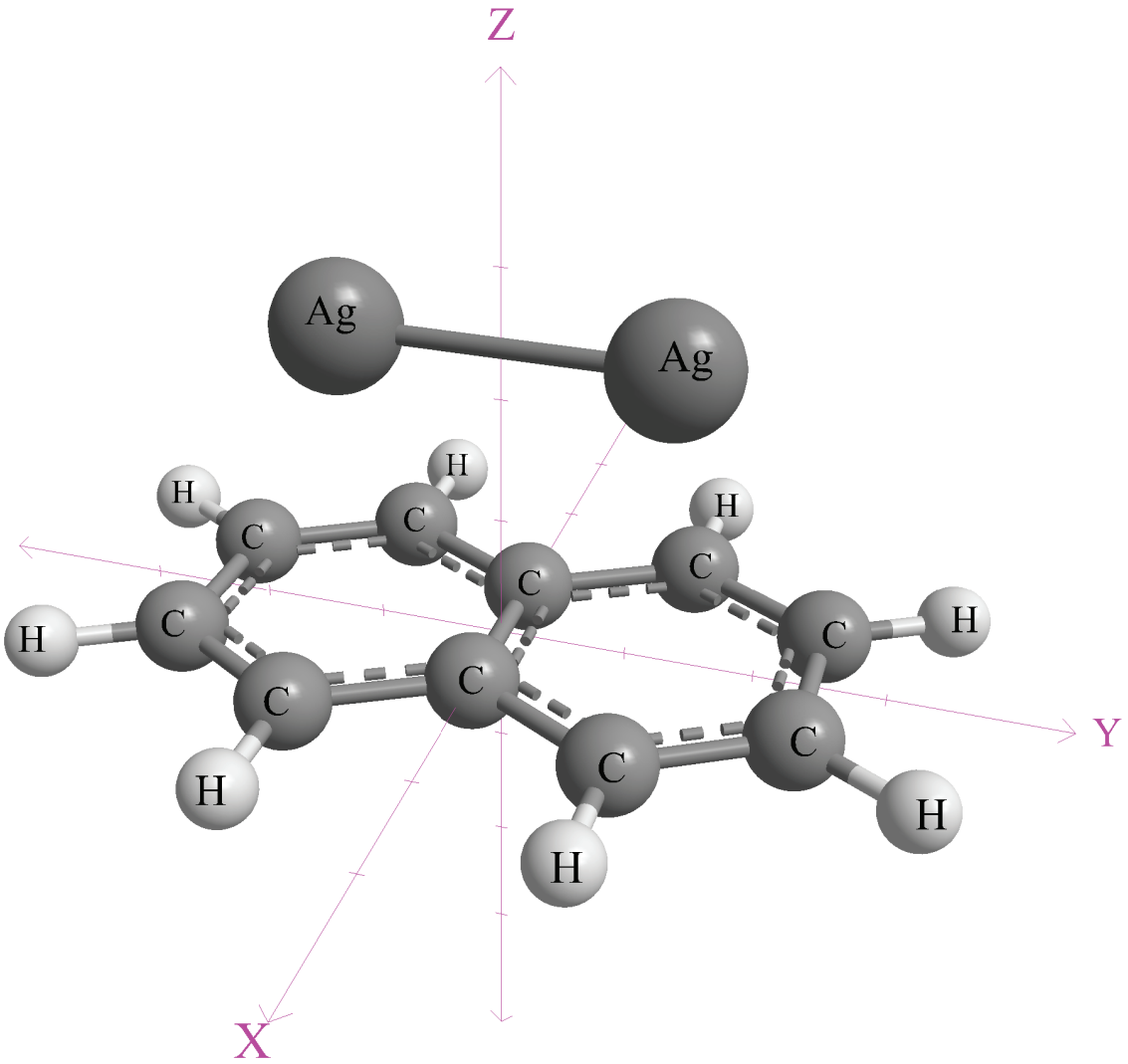

Figure 4.2: Schematic representation of one of the silver–naphthalene clusters studied. The other two examined clusters have the silver dimer co-linear with the x-axis, and the z-axis.

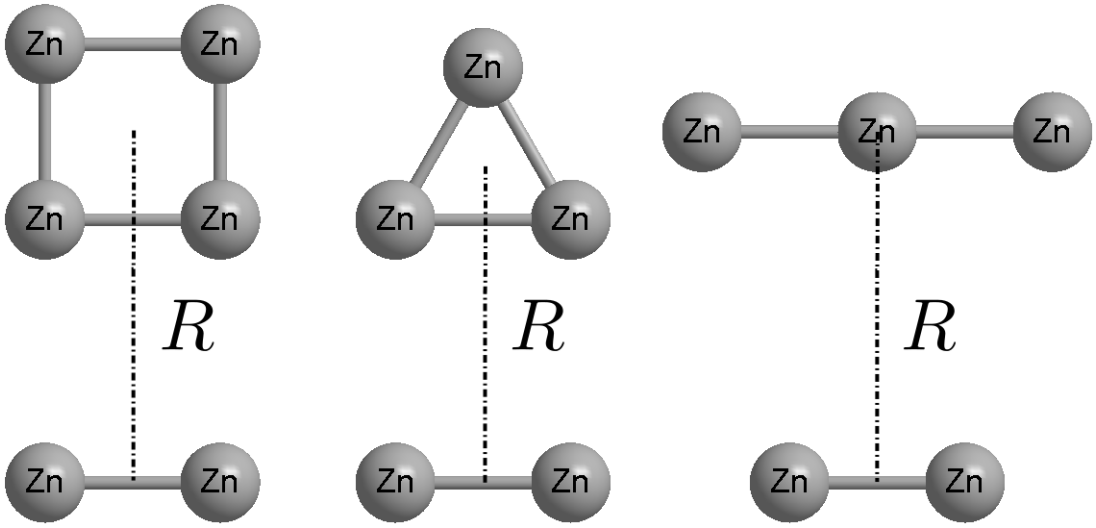

Figure 4.3: Schematic representation of the volatile metal clusters studied. The cadmium and mercury clusters possess an analogous structure. The intermolecular distance R is measured between the centers of mass of the monomers.

4.2 Theoretical Model

Based on their origin, the interactions occurring in the studied systems can be divided into two classes. At short intermolecular distances, the most important contributions stem from wave function overlap, and the exchange forces due to the antisymmetrization of the total wave function. At distances where these exponentially decaying forces can be neglected, the polarization approximation can be used to represent the total interaction potential V as a power series

$$V = \sum_i \frac{C_i}{R^i}, \tag{4.1}$$

where the coefficients C_i are in general functions of the orientation of the system, and the electric properties of the monomers, such as multipole moments or polarizabilities. For the interactions between two homonuclear diatomic molecules, the angular variations in the potential can be described via coupled spherical harmonic functions as[118–121]

$$V(R, \theta_1, \theta_2, \varphi) = \sum_{l_1, l_2, l} V_{l_1, l_2, l}(R) G_{l_1, l_2, l}(\theta_1, \theta_2, \varphi), \tag{4.2}$$

where the coordinates θ_1, θ_2, and φ are defined as in fig. 4.1. The coupled spherical harmonics are calculated as

$$\begin{aligned} G_{l_1, l_2, l}(\theta_1, \theta_2, \varphi) = & \frac{4\pi i^{l_1 - l_2 - l}}{\langle l_1, 0, l_2, 0 | l, 0 \rangle \sqrt{2l_1 + 1}\sqrt{2l_2 + 1}} \\ & \sum_{m=-\min(l_1, l_2)}^{\min(l_1, l_2)} Y_{l_1}^{(m)}(\theta_1, \varphi) Y_{l_2}^{(-m)}(\theta_2, 0) \langle l_1, m, l_2, -m | l, 0 \rangle , \end{aligned} \tag{4.3}$$

where $\langle l_1, m, l_2, -m | l, 0 \rangle$ is a Clebsch–Gordan coefficient,[76] and the functions $Y_l^{(m)}$ are the regular spherical harmonic functions. In the present form, the G functions are undefined for odd values of $l_1 + l_2 + l$, but such terms do not arise in the cases

studied due to the high symmetry of the dimers.[113] The normalization is such that $|G| = 1$ when the local and global axes are aligned, i.e., $\theta_1 = \theta_2 = \varphi = 0$.

As the long-range interaction potential physically arises form the various Coulombic interactions, the G functions can be used to describe them. In general, *any* scalar function depending on the relative orientation of two molecules, described by the Euler angles Ω_1 and Ω_2, can be expanded in terms of the complete set of functions[113]

$$S^{k_1,k_2}_{l_1,l_2,l} = i^{l_1-l_2-l} \sum_{m_1,m_2,m} \begin{pmatrix} l_1 & l_2 & l \\ m_1 & m_2 & m \end{pmatrix} D^{(l_1)}_{m_1,k_1}(\Omega_1)^* D^{(l_2)}_{m_2,k_2}(\Omega_2)^* C_{l,m}(\theta_R, \phi_R), \quad (4.4)$$

where $D^{(l_1)}_{m_1,k_1}(\Omega_1)$ is a Wigner rotation matrix element,[76] and $C_{l,m}(\theta_R, \phi_R)$ is a Racah spherical harmonic function[76] in terms of the orientation of the intermolecular vector $\mathbf{R}$. Symmetry considerations can be used to prove that the nonzero values of k_1 or k_2 are not required to describe the interactions between linear molecules, and odd values of l_1 or l_2 are unnecessary for centrosymmetric molecules.[113] In the latter case, it is more convenient to consider the functions

$$\bar{S}^{k_1,k_2}_{l_1,l_2,l} = \begin{pmatrix} l_1 & l_2 & l \\ 0 & 0 & 0 \end{pmatrix}^{-1} S^{k_1,k_2}_{l_1,l_2,l}, \quad (4.5)$$

normalized to $|\bar{S}^{k_1,k_2}_{l_1,l_2,l}| = 1$ if all angles vanish. In this form, the S functions can be used to describe the intermolecular interaction operator in the local axis system as[70]

$$H' = \sum_{l_1,l_2} \sum_{k_1,k_2} \begin{pmatrix} l_1 + l_2 \\ l_1 \end{pmatrix} \frac{\hat{\xi}^A_{l_1,k_1} \hat{\xi}^B_{l_2,k_2}}{R^{l_1+l_2+1}} \bar{S}^{k_1,k_2}_{l_1,l_2,l_1+l_2}. \quad (4.6)$$

For the description of the long-range interactions between a pair of homonuclear dimers, the functions $S^{0,0}_{l_1,l_2,l}$ with even values of $l_1 + l_2 + l$ are thus the only ones required, and if the intermolecular vector $\mathbf{R}$ is oriented along the global z-axis, then $\theta_R = \phi_R = 0$, and the normalized S functions reduce to the G functions in eq. (4.3).

As for the interactions relevant to this thesis, it can be seen from eq. (4.6) that the orientation dependent multipole–multipole interaction between two dimers can be expressed as

$$E_{\xi^A_{l_1,0}\xi^B_{l_2,0}}(R, \theta_A, \theta_B, \varphi) = \begin{pmatrix} l_1 + l_2 \\ l_1 \end{pmatrix} \frac{\xi^A_{l_1,0} \xi^B_{l_2,0}}{R^{l_1+l_2+1}} G_{l_1,l_2,l_1+l_2}(\theta_A, \theta_B, \varphi), \quad (4.7)$$

since a dimer can only have one permanent multipole moment of any order.[80] The leading order dispersion interaction between dimers has a slightly more complicated form[70,113]

$$\begin{aligned} E^{(6)}_{\text{disp}}(R, \theta_A, \theta_B, \varphi) = -\frac{C_6}{R^6} \Bigg[& 1 + \gamma_{2,0,2} G_{2,0,2} + \gamma_{0,2,2} G_{0,2,2} \\ & + \gamma_{2,2} \left(\frac{1}{15} G_{2,2,0} + \frac{2}{21} G_{2,2,2} + \frac{36}{35} G_{2,2,4} \right) \Bigg], \end{aligned} \quad (4.8)$$

where $G_{l_1,l_2,l} \equiv G_{l_1,l_2,l}(\theta_A, \theta_B, \varphi)$, and the dispersion coefficients are defined in eqs. (3.50) to (3.53). Similar expansions are possible for the induction energy contributions,[113] but in the cases studied this thesis, these effects were found to be negligible, and have mostly been ignored. The leading-order induction contribution between homonuclear dimers is the quadrupole–induced dipole interaction, whose magnitude decreases as R^{-8}, i.e., 2–3 orders of magnitude faster than the most important electrostatic and dispersion terms, which dominate the interactions.

4.3 Intermolecular Interaction Tensor

In Chapter 3 it was shown how the intermolecular interaction tensor T can be used to describe all of the long-range intermolecular interactions via perturbation theory. In Article IV, a novel formula for this tensor was presented as a result of considerations involving combinatorics[122] and the geometric Clifford algebra.[123,124] The derived formula allows the T tensor to be represented in a general vector form, applicable to both the Cartesian and the spherical bases. The expression obtained is suitable for both numerical and symbolic analyses, and offers a simple route to the equations governing the intermolecular interactions in a form which combines the advantageous properties of the Cartesian and spherical representations.

The Cartesian form of the T tensor in eq. (3.34) is succinct, but not well suited to all purposes. The idea of the approach presented in Article IV is to utilize this simple equation to build a more general representation, applicable in a wider context. Instead of calculating the derivatives only with respect to the Cartesian axes, the Clifford algebra definition of the directional vector derivative is employed. The derivative of a scalar function F of a vector variable $\mathbf{x}$ in the direction of the vector $\mathbf{a}$ is defined as[124]

$$\nabla_{\mathbf{a}} F(\mathbf{x}) \equiv \mathbf{a} \cdot \nabla F(\mathbf{x}) = \lim_{\tau \to 0} \frac{F(\mathbf{x} + \tau \mathbf{a}) - F(\mathbf{x})}{\tau}, \tag{4.9}$$

if the limit exists. This definition allows the derivatives to be taken in the direction of arbitrary vectors, but the downside is that the symbolic calculation of high-order directional derivatives might be challenging.

The explicit computation of high-order symbolic derivatives can be circumvented by adopting the multivariate Faà di Bruno formula for the generalization of the chain rule for higher derivatives.[122] If $y = y(x_1, x_2, \ldots, x_n)$ then

$$\frac{\partial^n}{\partial x_1 \partial x_2 \cdots \partial x_n} f(y) = \sum_{\pi \in P} f^{(|\pi|)}(y) \prod_{K \in \pi} \frac{\partial^{|K|} y}{\prod_{i \in K} \partial x_i}, \tag{4.10}$$

where P is the set of all partitions of the set $\{1, 2, \ldots, n\}$ and $|X|$ is the cardinality of the set X. For the interaction between two molecules A and B, with their centers of mass respectively located at points $\mathbf{A}$ and $\mathbf{B}$, the T tensor is essentially composed of derivatives of the function $1/R$, where $R = |\mathbf{R}| = |\mathbf{A} - \mathbf{B}|$. It is thus advantageous to apply the Faà di Bruno formula to the vector functions $y = y(\mathbf{R}) = \mathbf{R}^2 = R^2$ and $f(R) = 1/\sqrt{R}$, so that $f(y) = 1/R$, since $R > 0$.

The kth order derivatives of the function $f(y)$ can be calculated based on mathematical induction, and the required directional vector derivatives of the function $y(\mathbf{R})$ can be obtained directly from the definition in eq. (4.9), as detailed in Article IV. An important aspect to notice is that the function $y(\mathbf{R})$ has nonvanishing derivatives only up to second order, which considerably simplifies the calculations. After inserting the required formulas into eq. (4.10) and simplifying the result, the T tensor can be expressed in the form

$$T_X^{(n)}(\mathbf{R}) = \frac{1}{R^{n+1}} \sum_{\pi \in \mathcal{IP}} (-1)^{|\pi|} (2|\pi| - 1)!! \prod_{K \in \pi} \begin{cases} K_1 \cdot \hat{\mathbf{R}} & \text{if } |K| = 1 \\ K_1 \cdot K_2 & \text{if } |K| = 2 \end{cases} \tag{4.11}$$

where $\hat{\mathbf{R}} = \mathbf{R}/R$ is the unit vector in the direction of $\mathbf{R}$, $X = \{\boldsymbol{\alpha}, \boldsymbol{\beta}, \ldots, \boldsymbol{\nu}\}$ indicates the set of vectors in the direction where the derivatives are taken, and n is the number of elements in X, $n = |X|$. The permutations $\mathcal{IP}$ of X over which the summation is

performed, are the so-called involution permutations,[125] which possess the property of being their own inverses. In general, only a small subset of all permutations have this property, which further facilitates the calculations.

Article IV demonstrates various methods to calculate the T tensor and the permutations required, along with potential applications for the formulas. Particular attention is given to the vector formulation of the long-range dimer–dimer interactions between coinage metal and hydrogen clusters. For the quadrupole–quadrupole energy $E_{\Theta\Theta}$ between two homonuclear dimers, eq. (4.11) can be used used to obtain the formula

$$E_{\Theta\Theta} = \frac{3\Theta^A\Theta^B}{4R^5}\left[5r_{\mathbf{z}_A}^2\left(7r_{\mathbf{z}_B}^2-1\right)-5r_{\mathbf{z}_B}^2-20r_{\mathbf{z}_A}r_{\mathbf{z}_B}c_{\mathbf{z}_A,\mathbf{z}_B}+2c_{\mathbf{z}_A,\mathbf{z}_B}^2+1\right], \quad (4.12)$$

where $\mathbf{z}_A$ and $\mathbf{z}_B$ are body fixed unit vectors in the local z direction, $r_{\mathbf{z}_X} = \hat{\mathbf{R}}\cdot\mathbf{z}_X$ ($X = A$ or $X = B$), and $c_{\mathbf{z}_A,\mathbf{z}_B} = \mathbf{z}_A\cdot\mathbf{z}_B$. If the coordinate system is fixed as in fig. 4.1, the dot products are

$$r_{\mathbf{z}_X} = \cos\theta_X \quad (4.13)$$

$$c_{\mathbf{z}_A,\mathbf{z}_B} = \cos\theta_A\cos\theta_B+\sin\theta_A\sin\theta_B\cos\varphi, \quad (4.14)$$

which yield the explicit form of the quadrupole–quadrupole interaction energy, given in eq. (3.43), when plugged back into eq. (4.12). The dispersion energy can be treated similarly, and the result for two dimers is

$$\begin{aligned}E_{\text{disp}}^{(6)} = -\frac{C_6}{R^6}\Bigg[1+\frac{1}{2}\gamma_{2,0,2}\left(3r_{\mathbf{z}_A}^2-1\right)+\frac{1}{2}\gamma_{0,2,2}\left(3r_{\mathbf{z}_B}^2-1\right)\\ +\frac{1}{2}\gamma_{2,2}\left(c_{\mathbf{z}_A,\mathbf{z}_B}^2-6r_{\mathbf{z}_A}r_{\mathbf{z}_B}c_{\mathbf{z}_A,\mathbf{z}_B}-r_{\mathbf{z}_A}^2\left(1-9r_{\mathbf{z}_B}^2\right)-r_{\mathbf{z}_B}^2\right)\Bigg],\end{aligned} \quad (4.15)$$

where the γ coefficients are as defined in eqs. (3.50) to (3.53). The equivalence to eq. (4.8) can be seen by inserting the definitions for the dot products in eqs. (4.13) and (4.14). A further comparison to eq. (4.8) yields the following vector representations of some of the low-order G functions defined in eq. (4.3).

Table 4.1: Vector Representations of Certain Low-Order G Functions

G function[a]	Vector Form
$G_{0,0,0}$	1
$G_{2,0,2}$	$\frac{1}{2}\left(3r_{\mathbf{z}_A}^2-1\right)$
$G_{2,2,0}$	$\frac{1}{2}\left(3c_{\mathbf{z}_A,\mathbf{z}_B}^2-1\right)$
$G_{2,2,2}$	$\frac{3}{2}\left(r_{\mathbf{z}_A}^2+r_{\mathbf{z}_B}^2+c_{\mathbf{z}_A,\mathbf{z}_B}^2-3r_{\mathbf{z}_A}r_{\mathbf{z}_B}c_{\mathbf{z}_A,\mathbf{z}_B}\right)-1$
$G_{2,2,4}$	$\frac{1}{8}\left[5r_{\mathbf{z}_A}^2\left(7r_{\mathbf{z}_B}^2-1\right)-5r_{\mathbf{z}_B}^2-20c_{\mathbf{z}_A,\mathbf{z}_B}r_{\mathbf{z}_B}r_{\mathbf{z}_A}+2c_{\mathbf{z}_A,\mathbf{z}_B}^2+1\right]$

[a] The corresponding G functions with indices l_1 and l_2 swapped are obtained by swapping $r_{\mathbf{z}_\mathrm{A}}$ and $r_{\mathbf{z}_\mathrm{B}}$.

As the previous examples indicate, the combinatorial formulation of the interaction tensor can be utilized to describe various intermolecular forces in a convenient fashion using vector calculus. This approach facilitates the change of basis or rotation convention, and the treatment of rigid motions, as detailed in Article IV. The equation is also presented in a form which does not require the explicit calculation of high-order vector derivatives, as opposed to, for example, the expression presented in eq. (3.26).

4.4 Multipole Moments and Polarizabilities

The multipole moments and polarizabilities describing the electric properties of the studied molecules can be calculated from the total interaction potential energy surface by means of, for example, eq. (4.7). However, the quantities in question can also be obtained via a simpler method based on a perturbation expansion of the total energy and its gradients, presented in eqs. (3.27) and (3.28). This technique is known as the finite field method,[81,126–128] and it involves calculating numerical derivatives of the total energy in the presence of a weak perturbation $\lambda\hat{\xi}$, where $\hat{\xi}$ is a multipole moment and λ is a parameter. Should the wave function Ψ satisfy the Hellmann–Feynman theorem,[50,51] the derivative of the energy will correspond to the expectation value of the multipole moment,

$$\frac{\partial E}{\partial \lambda} = \langle \Psi | \, \hat{\xi} \, | \Psi \rangle \,, \tag{4.16}$$

in the limit $\lambda \to 0$. Second derivatives can similarly be used to calculate polarizabilities.[81,128–130]

The electronic structure methods used in this thesis, the Møller–Plesset perturbation theory and the coupled cluster theory, are not variational, so eq. (4.16) does not exactly hold for them, although the discrepancy becomes smaller as the quality of the approximate wave function increases, because the Hellmann–Feynman theorem holds for the exact wave function.[53] Despite the differences between the derivatives and the expectation values, the finite field method has been extensively used,[131] and it has been argued that the derivative method resembles the physical experiment more, and should be preferred.[53,81] In this thesis, the calculations are mostly performed at the CCSD(T) level, where the multipole moments cannot be calculated as expectation values, as there is no CCSD(T) wave function, but even in this case, the finite field method can be used to estimate the desired moment. The downside is that this technique is susceptible to numerical noise, but if factors such as the numerical derivative formulas and field strengths are carefully chosen, reliable results can be obtained in a straightforward fashion.[128,130–132]

The quadrupole moments Θ, hexadecapole moments Φ, and polarizabilities α, calculated for the coinage and volatile metal dimers based on the finite field method, are presented in table 4.2. For the coinage metals, the polarizabilities were not calculated by the finite field method, but the results of Saue and Jensen[133] were used. These values are reported in table 4.2 for completeness. The quadrupole moments for the larger volatile metal systems—the trimer, triangle, and square, depicted in fig. 4.3—are presented in table 4.3.

Table 4.2: Calculated Values for the Quadrupole and Hexadecapole Moment and Polarizability Tensor Components[a]

Molecule	Θ	Φ	$\alpha_{\parallel}$	$\alpha_{\perp}$
Cu_2	5.8160	56.9952	123.8	81.9
Ag_2	6.3194	74.9375	156.2	97.0
Au_2	6.5719	116.4838	114.2	65.7
Zn_2	−0.1494	−10.1507	92.26	71.37
Cd_2	−0.3596	−19.0751	121.66	85.50
Hg_2	−0.4845	−15.0842	91.75	63.40

[a] All values are given in atomic units. For the quadrupole moment 1 a.u. = $4.486551484 \times 10^{-40}\,\mathrm{C\,m^2}$, for the hexadecapole moment 1 a.u. = $1.256362373 \times 10^{-60}\,\mathrm{C\,m^4}$, and for the polarizability 1 a.u. = $1.648777273 \times 10^{-41}\,\mathrm{C^2\,m^2\,J^{-1}}$.[134] The polarizability values for the coinage metal dimers were calculated by Saue and Jensen.[133]

Table 4.3: Calculated Values for the Quadrupole Moments of the Volatile Metal Clusters.[a]

System	Trimer	Triangle	Square
Zn	−0.3258	0.1616	0.2477
Cd	−0.8234	0.3626	0.5730
Hg	−1.1522	0.5282	0.8017

[a]All values are given in atomic units.

In order to obtain reliable results, various finite field schemes were utilized in the calculations, depending on the system and the calculated property. The derivatives were calculated by means of three- to seven-point numerical central differences formulas,[135] and the field strength of the perturbation was between $1.0\times10^{-3}\,E_\mathrm{h}/(ea_0)$ and $1.0\times10^{-6}\,E_\mathrm{h}/(ea_0)$ ($E_\mathrm{h} = 4.359744650\times10^{-18}\,\mathrm{J}$, $e = 1.6021766208\times10^{-19}\,\mathrm{C}$, $a_0 = 0.52917721067\times10^{-10}\,\mathrm{m}$).[134] The utilized parameter values were selected based on numerical stability and by comparing the finite field results to the corresponding operator eigenvalues at the Hartree–Fock level. The values for the various electric properties agree well with other computational results,[136–138] and can therefore be used to accurately represent the corresponding long-range interaction terms.

4.5 Dispersion Interactions

In this thesis, the dispersion interactions play an instrumental role. Despite the many different schemes developed to account for them,[25–34] the accurate calculation of the van der Waals forces can present difficulties in complicated systems. In the articles included in this thesis, a pair-potential model for the dispersion interactions is presented and applied to non-covalent interactions in the studied clusters. For the volatile metal systems, the vdW interactions of larger clusters are accurately modeled based on interatomic dispersion coefficients calculated from small reference systems. Results are also obtained for orientation averaged dispersion energies, which the pair-pair potential approach is able to describe to a remarkable degree.

Besides the pair-potential approach, Article IV presents a study of the potential energy surface and the long-range forces of coinage metal and hydrogen clusters in the confines of the common molecular multipole expansion, performed via application of the interaction formulas presented in sections 4.2 and 4.3.

Coinage Metal–Hydrogen Clusters

In Article IV, the long-range forces, and especially dispersion interactions were studied in H_2–H_2 and M_2–H_2 (M = Cu, Ag, Au) clusters. The desired interaction coefficients were calculated from least-squares fits to the potential energy surface, computed at large intermolecular distances.

The most important factors determining the long-range interaction energy landscape of the studied clusters are the dispersion and quadrupole–quadrupole forces. In terms of the vector approach of section 4.3, the relevant formulas are given in eqs. (4.12) and (4.15). In the case of the hydrogen clusters, the corresponding geometry terms yield an accurate representation of the long-range PES, as can be seen from fig. 4.4. All of the interaction terms are well defined and linear on the logarithmic scale, indicating the validity of the inverse power series expansion at the studied distances. The results for the hydrogen–coinage metal clusters, detailed in Article IV, are similar, although some higher-order fitting terms were necessary to capture all the relevant interactions.

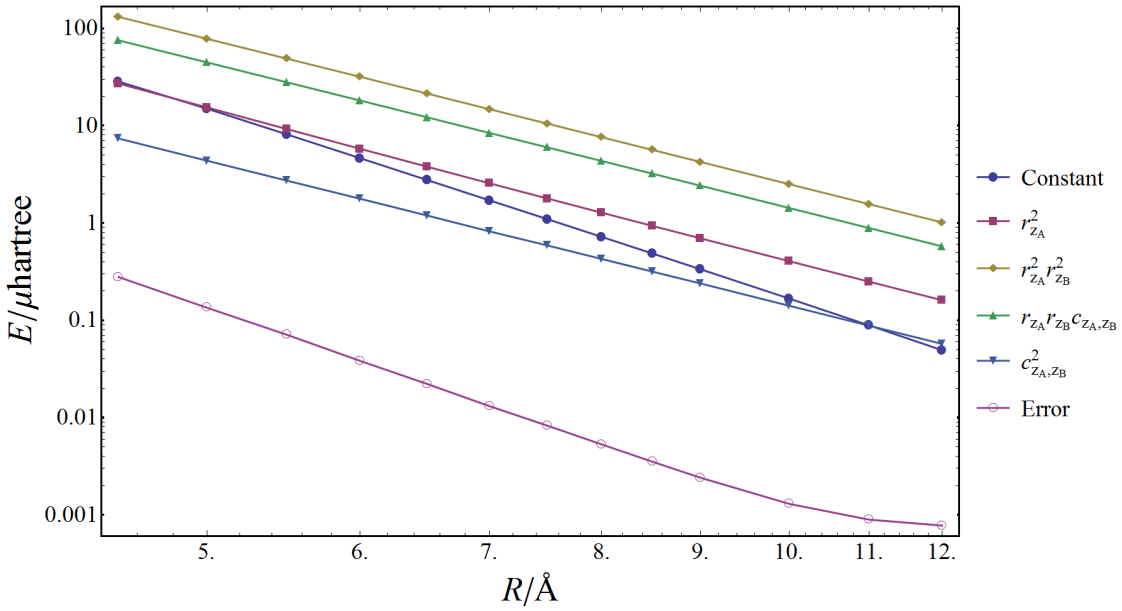

Figure 4.4: The long-range interaction potential energy fit for the H_2–H_2 cluster in a logarithmic scale, where R is the distance between the centers of mass of the dimers. The orientation dependence of the fit parameters is given in the legend. The error term is the one standard deviation error of the least-squares fit. The lines are guides for the eye. 1 hartree = $4.359744650 \times 10^{-18}$ J.[134]

By comparing the geometry dependence of the fitted PES terms to the equations governing the long-range intermolecular forces, the desired interaction parameters can be calculated based on the energy expansion presented in eqs. (4.2) and (4.3). By expressing the interactions in terms of the coupled spherical harmonic G functions, as accomplished in eqs. (4.7) and (4.8), the multipole moments and dispersion coefficients can be related to the fitting parameters. For example, in fig. 4.4, the constant term describes the part of the potential energy surface without any associated orientation dependence, i.e., the isotropic component, which is equal to the $V_{0,0,0}(R)$ term of the energy expansion in eq. (4.2). This term is related to the isotropic dispersion coefficients as

$$V_{0,0,0}(R) = \frac{C_6}{R^6} + \frac{C_8}{R^8} + \cdots , \tag{4.17}$$

and similar relations can also be written for the other interaction parameters, as described in Article IV.

The dispersion coefficients and multipole moments for the studied clusters were calculated based on the analysis described. For the H_2–H_2 system, all of the calculated parameters fell within 1% of the well known reference values,[120,121,139,140] which is an indication of the accuracy of the present approach. For the coinage metal–hydrogen clusters, the coefficients resulting from the analysis described are presented in table 4.4. The electronic structure calculations were performed at the CCSD(T) level, with the aug-cc-pVTZ-PP[141–144] basis set utilized for the coinage metal atoms. The effects of the basis set convergence were examined for the copper system. The energies were found to be converged, and the triple-ζ basis set was thus deemed sufficient for the calculations. The standard errors of the fits for the C_6 coefficients and the multipole moments were approximately 1% and 2%, respectively. The fits for the C_8 coefficients had a larger error of 10%, due to the steep distance dependence of this term, and the numerical instabilities related to the separation of tiny differences in the total energy. Despite these margins of error, the obtained coefficients are well

defined, and manage to reproduce the calculated PES to a satisfactory degree.

Table 4.4: Calculated Intermolecular Interaction Parameters for the Coinage Metal Containing Clusters[a]

M	$C_6^{(\mathrm{H_2M_2})}$	$C_8^{(\mathrm{H_2M_2})}$	$\Theta^{\mathrm{M_2}}$	$\Phi^{\mathrm{M_2}}$
Cu	94.67	5753	5.742	54.37
Ag	120.9	8241	6.298	70.78
Au	116.5	8962	6.535	116.1

[a] All values are in atomic units. For the C_6 constant $1\,\mathrm{a.u.} = 9.573436258 \times 10^{-80}\,\mathrm{J\,m^6}$, and for the C_8 constant $1\,\mathrm{a.u.} = 2.680835190 \times 10^{-100}\,\mathrm{J\,m^8}$.[134]

Pair-Potential Model

In the presented pair-potential model, the dispersion energy of a cluster is divided into interatomic contributions, each with a specific dependence on the system geometry, as exemplified in fig. 4.5. This procedure enables the total dispersion energy of the whole system to be written in terms of atomic dispersion coefficients, which are obtained from a least-squares fit to the computed potential energy surface of small model clusters. The obtained values can thereafter be used to calculate the dispersion interactions in larger systems, where the direct computation of the PES is prohibitively laborious.

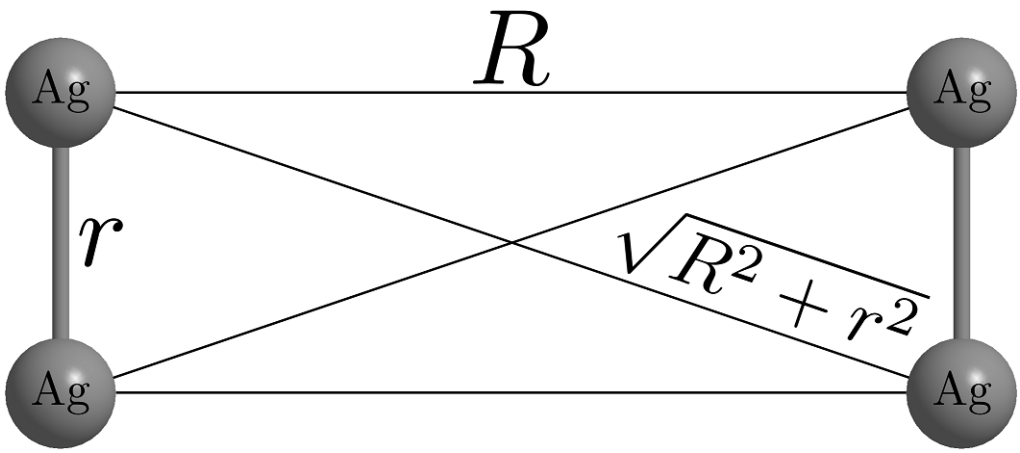

Figure 4.5: Schematic representation of the pair-potential dispersion energy model in a silver cluster. The solid black lines represent the contributing atom pairs. The bond length of the dimers is r, while R signifies the center-of-mass distance between them.

In the situation depicted in fig. 4.5, the lowest-order dispersion contribution is

$$E_{\mathrm{disp}}^{(6)} = -C_6^{(\mathrm{AgAg})} \left[2R^{-6} + 2\left(R^2 + r^2\right)^{-3} \right], \tag{4.18}$$

where $C_6^{(\mathrm{AgAg})}$ is the effective atom pair dispersion coefficient between two silver atoms. In general, the pair approximation can be written as

$$E_{\mathrm{disp}}^{(6)} = \sum_i C_6^{(i)} R_i^{-6}, \tag{4.19}$$

where the summation is over the contributing atom pairs, and expressed in terms of the atom–atom dispersion coefficients $C_6^{(i)}$ and distances R_i. An explicit expression applicable to planar dimer–dimer clusters of arbitrary orientation is presented in Article I.

In the articles included in this thesis, the interactomic dispersion coefficients have been obtained by the following procedure. First, the interaction energy of the metal clusters is calculated as a function of the intermolecular distance, and the electrostatic energy is subtracted at each point. As the induction contributions were found to be minimal, the remaining energy is mainly due to the dispersion effects, which are modeled by the pair-potential formula of eq. (4.19). Finally, the interatomic vdW coefficients are obtained as least-squares fitting parameters to the dispersion energy.

By examining the M_2–M_2 (M stands for Cu, Ag, Au, Zn, Cd, or Hg) metal systems at the CCSD(T)/aug-cc-pVTZ-PP [141–144] level, the $C_6^{(MM)}$ dispersion coefficients have been determined for several cluster orientations, specified via the angles depicted in fig. 4.1. The results, presented in table 4.5, have been obtained from the planar ($\varphi = 0$) configurations with $\theta_1 = \theta_2 = \theta$, while the considered intermolecular distances ranged from 10 to 35 Å (1 Å $= 10^{-10}$ m).

Table 4.5: The Calculated Atomic C_6 Coefficients for Group 11 and 12- Dimers[a]

θ	$C_6^{(CuCu)}$	$C_6^{(AgAg)}$	$C_6^{(AuAu)}$	$C_6^{(ZnZn)}$	$C_6^{(CdCd)}$	$C_6^{(HgHg)}$
0°	132.49 (28)	226.70 (46)	187.72 (26)	208.62 (41)	349.02 (79)	280.96 (146)
10°	139.92 (22)	236.09 (36)	205.26 (16)	209.39 (52)	350.50 (101)	280.08 (135)
20°	155.30 (8)	253.86 (19)	240.73 (18)	207.39 (79)	345.12 (141)	273.16 (126)
30°	164.68 (10)	263.45 (7)	261.60 (28)	201.05 (96)	332.18 (171)	261.39 (118)
40°	158.97 (19)	254.35 (28)	250.27 (27)	191.33 (91)	313.91 (167)	247.33 (102)
50°	142.31 (20)	231.39 (41)	216.42 (23)	181.13 (78)	294.83 (144)	233.65 (84)
60°	128.57 (22)	212.38 (48)	187.86 (19)	172.91 (65)	279.39 (121)	222.64 (70)
70°	128.23 (37)	212.04 (69)	187.51 (36)	167.64 (51)	269.68 (107)	215.70 (59)
80°	137.65 (64)	225.85 (106)	209.39 (87)	164.90 (41)	265.11 (102)	212.57 (53)
90°	143.35 (77)	234.19 (125)	222.84 (118)	164.04 (39)	263.90 (101)	211.76 (51)
Average	143.15	235.03	216.96	186.84	306.36	243.92

[a] The C_6 coefficients are expressed in eV Å^6 (1 eV $= 1.6021766208 \times 10^{-19}$ J) [134] and the angles in degrees. The uncertainties of the least-squares fits given in parentheses are one-standard errors in the least significant digit.

In Article I, the pair-potential method was also applied to the silver–naphthalene system, depicted in fig. 4.2. The procedure followed a similar approach undertaken earlier for the silver–benzene system. [145] The purpose was to obtain the silver–carbon dispersion coefficients, which might be used to model the non-covalent interactions in extended systems, such as Ag clusters adsorbing on a graphite surface. [146] However, this line of research was not followed in this thesis, as the focus of the subsequent articles shifted towards pure metal clusters. The calculations were performed at the spin component scaled second order Møller–Plesset perturbation theory (SCS-MP2) level, [147] which largely corrects [147,148] the overbinding associated with the regular MP2 method for certain complex systems. [149–151] The obtained $C_6^{(AgC)}$ dispersion coefficients for the orientations specified in fig. 4.2 ranged approximately from 51.5 to 96.0 eV Å^6, with an average value of 77.75 eV Å^6. Compared to the earlier findings, [145] the coefficients varied more with orientation, but the average value was still within 10% of the results obtained from the silver–benzene system.

The orientational variation of the interatomic C_6 coefficients is also evident in the metal systems, as can be seen from table 4.5. The angle dependence of the computed interatomic dispersion coefficients is shown in figs. 4.6 and 4.7. In both element groups, clear similarities can be seen in the shapes of the curves, although the volatile metals show a more tempered behavior. A factor likely to contribute to this effect is

that the volatile metal dimers are themselves dispersion dominated systems, where the atoms are more separated [152] compared to the coinage metal dimers. A further correspondence can be found in the relative magnitudes of the vdW parameters: in both groups, the ordering of the C_6 coefficients differs from the atomic number order of the elements, presumably due to the relativistic effects to polarizability. [153]

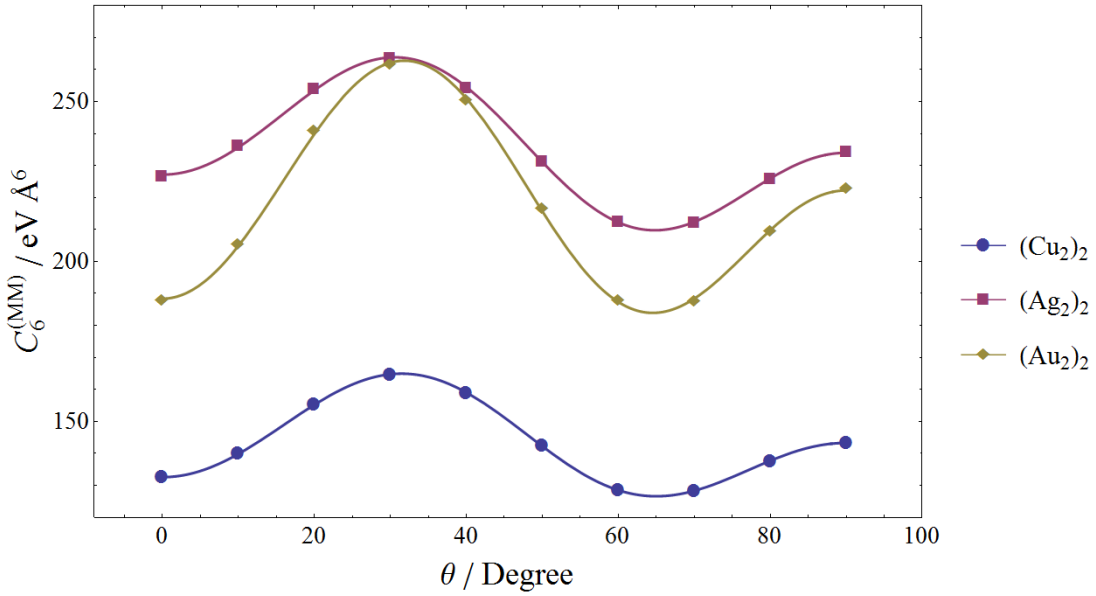

Figure 4.6: The calculated $C_6^{(\mathrm{MM})}$ (M = Cu, Ag, Au) coefficients for the different coinage metal clusters. The lines represent least-squares fits in terms of the G functions in eq. (4.3)

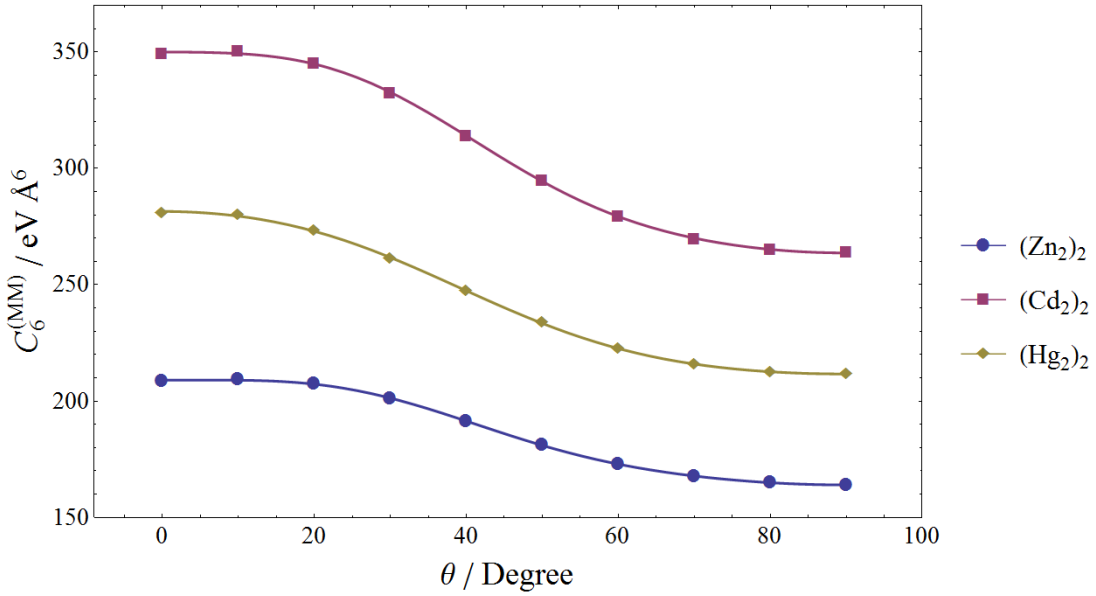

Figure 4.7: The calculated $C_6^{(\mathrm{MM})}$ (M = Zn, Cd, Hg) coefficients for the different volatile metal clusters. The lines represent least-squares fits in terms of the G functions in eq. (4.3)

The orientation dependence of the interatomic C_6 coefficients is well described in terms of the coupled spherical harmonic functions of eq. (4.3), as can be ascertained from figs. 4.6 and 4.7. A fit of this type has the additional advantage that it separates the interaction into constant and geometry dependent parts. The volatile metals studied in this thesis possess a closed valence shell, and values for their isotropic atomic

dispersion coefficients can also be obtained from direct calculations on the respective atom–atom systems. The results in table 4.6 show that the atomic coefficients thus obtained are in good agreement with the isotropic values obtained from the fits to the dimer–dimer systems. For both the coinage and volatile metal systems, the isotropic values are close to the average values of the calculated coefficients.

Table 4.6: Comparison of Group 11 and 12 Dispersion Coefficients[a]

Coefficient	Isotropic value	Average value	Atomic
$C_6^{(\mathrm{CuCu})}$	141.72	143.15	
$C_6^{(\mathrm{AgAg})}$	231.49	235.03	
$C_6^{(\mathrm{AuAu})}$	215.53	216.96	
$C_6^{(\mathrm{ZnZn})}$	178.77	186.84	175.16
$C_6^{(\mathrm{CdCd})}$	290.79	306.36	283.09
$C_6^{(\mathrm{HgHg})}$	231.35	243.92	222.18

[a]All values are in eV $\mathrm{\AA}^6$. The isotropic value refers to the constant term of the fits depicted in figs. 4.6 and 4.7 and the average value to the average of the dispersion coefficients reported in table 4.5.

4.6 Applications

The interatomic dispersion coefficients presented in this thesis can be utilized in various situations. In Article II, the pair-potential model is applied to the computation of orientation averages of the dispersion interactions in the dimer–dimer volatile metal systems. In Article III, the obtained parameters are employed in calculating the vdW interactions in larger volatile metal clusters. The results indicate that in both cases, the atomic dispersion coefficients yield an accurate representation of the studied interactions.

Orientation Averages

In complicated systems, or in cases where the molecules are free to rotate, an orientation average of the dispersion interactions is often of particular interest. The simple unweighted orientation averages of the dispersion energy in the volatile metal clusters were calculated in Article II. In terms of molecular coefficients, the dispersion interactions can be expressed as an expansion in the inverse powers of the intermolecular distance, as in eq. (4.1). In case of the orientation averages of the dimer–dimer systems, the coefficients of this expansion are linear combinations of the molecular isotropic dispersion coefficients, and additional terms due to polarizability anisotropy, such as the γ terms in eq. (3.49). For the rest of this subsection, this type of expansion is referred to as 'molecular', in order to distinguish it from the pair-potential expansion in terms of atomic dispersion coefficients.

The situation is different, if the energy expansion is performed in terms of the atomic dispersion coefficients via the pair-potential model. For the geometries studied in Article II, i.e., those resulting from setting $\varphi = 0$, and $\theta_1 = \theta_2 = \theta$ in fig. 4.1, this model reduces to

$$E_{\mathrm{disp}} = -\sum_n C_{2n} \left[2R^{-2n} + \left(r^2 + R^2 + 2rR\cos\theta \right)^{-n} + \left(r^2 + R^2 - 2rR\cos\theta \right)^{-n} \right], \tag{4.20}$$

where r is the monomer bond length, and the energy is characterized by an integer $n \geq 3$. For example, if $\theta = 90°$, the situation is as depicted in fig. 4.5, and the first term in eq. (4.20) reduces to eq. (4.18).

The orientation average of the pair-potential model behaves differently compared to the expansion in terms of the molecular coefficients. Each term in the molecular expansion has a specific distance dependence, but averaging the general term in eq. (4.20) over the angle θ results in a series

$$\bar{E}_{\text{disp}}^{(2n)} = -2C_{2n}\left[R^{-2n} + \sum_{k=0}^{\infty} \frac{\Gamma(k+n)^2}{(k!)^2\Gamma(n)^2}\frac{r^{2k}}{R^{2k+2n}}\right], \tag{4.21}$$

where Γ is the gamma function. In closed form, this series can be expressed either in terms of the hypergeometric function ${}_2F_1$, or the Legendre polynomial of order n, as shown in Article II. Based on eq. (4.21), the asymptotic long-distance expansion for the leading order dispersion energy term in the pair-potential model is

$$\bar{E}_{\text{disp}}^{(6)} = -C_6\left(\frac{4}{R^6} + \frac{18r^2}{R^8} + \frac{72r^4}{R^{10}} + \cdots\right), \tag{4.22}$$

which contains contributions from various R terms, as opposed to the clear-cut R^{-6} dependence of the molecular expansion.

The two previously discussed expansions were compared in their ability to model the calculated orientation averages of the volatile metal clusters. The expansions were fitted in the least-squares sense to the computed dispersion energies, and the fit residuals and goodness-of-fit measures were compared for the two models. The results are presented in fig. 4.8 for the Zn_2–Zn_2 clusters.

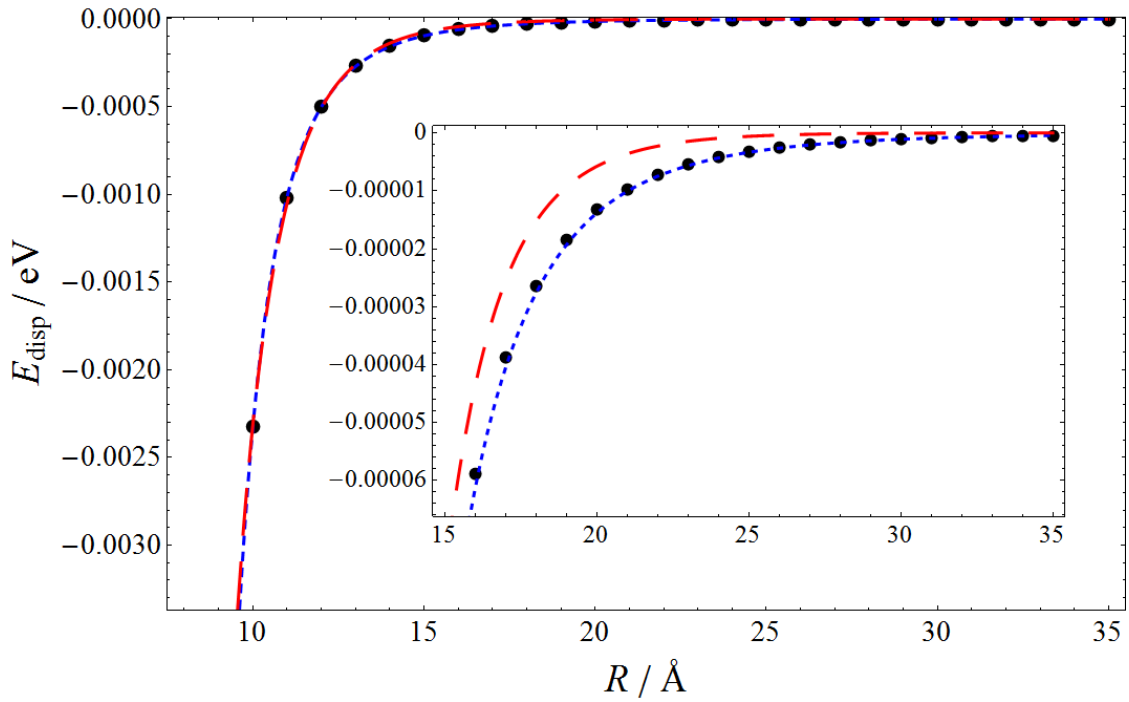

Figure 4.8: Least-squares fits of the pair-potential model $\bar{E}_{\text{disp}}$ (dotted blue curve) and the molecular expansion (dashed red curve) to the orientation averaged dispersion energy of the $Zn_2 - Zn_2$ system.

The fits in fig. 4.8 indicate that the pair-potential model is able to describe the average dispersion energy to a more satisfactory degree, where as the molecular

expansion model shows clear deviations from the calculated points. This behavior is due to the higher impact of the close-range points, and is largely corrected by neglecting some of them. The pair-potential expansion, on the other hand, is virtually unaffected by this procedure, and can hence describe the orientation averaged dispersion energy more reliably over a wider range of distances than the molecular expansion model. This result is surprising, since the latter should more closely describe the actual physical phenomenon, but it is possible that the asymptotic expansion of the pair-potential model, eq. (4.21), allows for a more concise representation of some higher-order terms not present in the truncated molecular expansion.

Larger Metal Clusters

In Article III, the dispersion coefficients presented in table 4.5 were utilized to determine the van der Waals interactions of some larger metal systems, i.e., the Zn, Cd, and Hg clusters, whose structures are presented in fig. 4.3. The procedure employed consisted of partitioning the total dispersion interaction into dimer contributions, which were then modeled by using the previously computed coefficients. The process is schematically depicted in fig. 4.9.

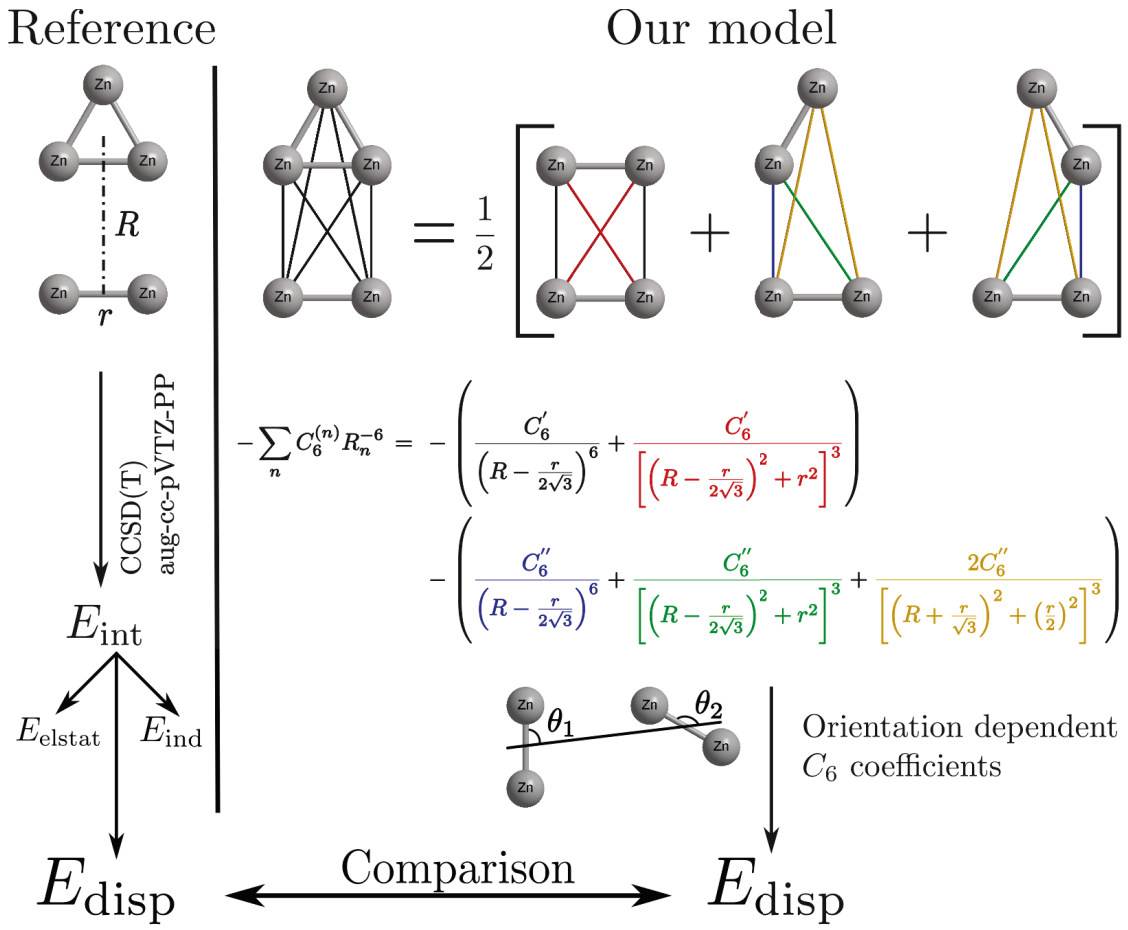

Figure 4.9: Schematic representation of the atomic pair potential model applied to the dimer–triangle cluster. The colors are used to label different types of atomic pair interactions, and the dispersion energy terms resulting from them. The factor $\frac{1}{2}$ is included to avoid double counting.

In order to properly resolve the dispersion forces, a more flexible model is required for the pairwise interactions. The vdW coefficients in table 4.5 were calculated for

geometries with $\theta_1 = \theta_2 = \theta$ (see figs. 4.1 and 4.9), but in the present application, nonparallel orientations appear as well, and the fits in fig. 4.7 need to be augmented in order to account for this fact. In practice, the most important terms in the fits are linear combinations of functions of type $\cos(n\theta)$, where n is an even integer. To include nonparallel configurations, the calculations therefore utilized the simplified formula

$$C_6(\theta_1, \theta_2) = \bar{C}_6 + \frac{\Delta C_6}{2}\left[\cos(2\theta_1) + \cos(2\theta_2)\right], \tag{4.23}$$

where $\bar{C}_6$ is the average value, and ΔC_6 is the difference between the maximum and the average of the dispersion coefficient (see fig. 4.7). The formula in eq. (4.23) also implicitly depends on the separation of the molecules, as the angles in general change with intermolecular distance.

For the parallel orientations, eq. (4.23) closely resembles the fits in fig. 4.7. As a test case for the nonparallel orientations, the atomic dispersion coefficients $C_6^{(\mathrm{MM})}$ ($\mathrm{M} = \mathrm{Zn}, \mathrm{Cd}, \mathrm{Hg}$) were calculated for the T-configuration of the dimers ($\theta_1 = 0°, \theta_2 = 90°$), and compared to the values given by eq. (4.23). The results in Article III indicate that the two methods were in good agreement: the *ab initio* calculated dispersion coefficients were about 1 to 2 percent smaller than the values calculated based on eq. (4.23).

The *ab initio* calculated dispersion energies for the studied metal clusters were compared to the values given by the pair potential model, and the dispersion corrections given by the DFT-D3 method of Grimme *et al.*[29] The results for the dimer–triangle case, depicted in fig. 4.9, are presented in fig. 4.10. The comparison indicates that the pair-potential method is able to faithfully reproduce the calculated dispersion energies; even the isotropic values from table 4.6 perform remarkably well. The anisotropic corrections form eq. (4.23) improve the results slightly, the effect being greatest for the dimer–trimer clusters (see fig. 4.3).

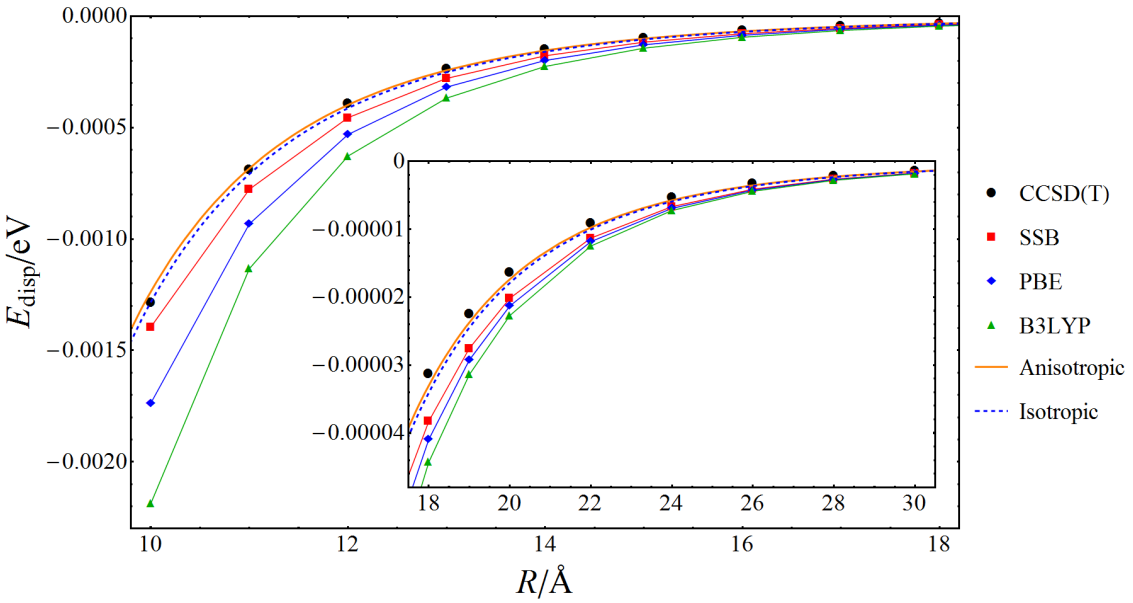

Figure 4.10: Dispersion energy in the Zn dimer – triangle cluster compared with calculations based on the presented method and various DFT-D3 results.

The DFT-D3 dispersion corrections for the various functionals, depicted in fig. 4.10, do not yield as accurate results, although it should be noted that the comparison is biased in favor the pair-potential method, since the same level of theory was used

to calculate both the reference points and the interatomic dispersion coefficients. However, it can be ascertained that, in the cases studied, the pair-potential method is able to give reliable results for the dispersion energies without any additional electronic structure calculations. Furthermore, the accuracy of the energies thus obtained is in accordance with the level of theory used to calculate the dispersion coefficients.

In Article III, the approach presented in this thesis was compared with two other pair-potential methods—the extended Lennard-Jones (ELJ) model of Pahl *et al.*,[154] and the Tang–Tonnies (TT) potential model.[155] The comparison was performed for the mercury clusters, and the results for the dimer–trimer system are shown in fig. 4.11. All of the models yield results in reasonable accordance with one another, although different methods were utilized to obtain the potentials. The ELJ model is the result of CBS/CCSD(T)+SO level calculations on the mercury dimer, while the TT method relies on theoretical and experimental results for the dynamic polarizability of mercury. In both of these methods, the value[155] $C_6^{(\mathrm{HgHg})} = 234.2\,\mathrm{eV\,\AA^6}$ has been adopted for the dispersion coefficient, which is in good agreement with the isotropic value $C_6^{(\mathrm{HgHg})} = 231.35\,\mathrm{eV\,\AA^6}$ from table 4.6.

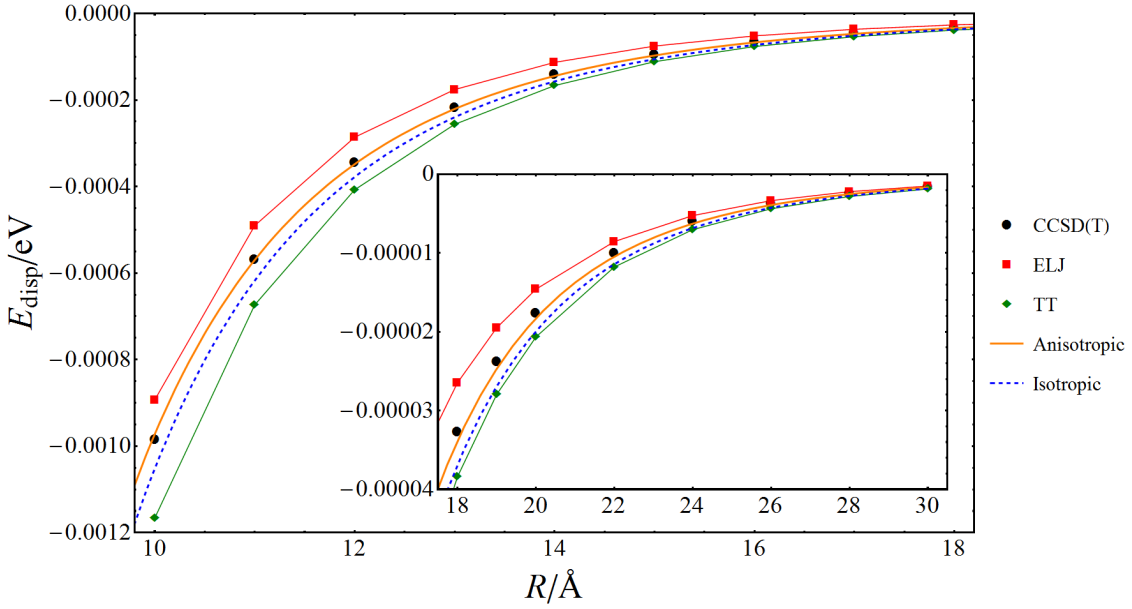

Figure 4.11: Dispersion energy in the Hg dimer–trimer cluster compared with calculations based on the presented approach, the extended Lennard-Jones (ELJ) model,[154] and the Tang–Tonnies (TT) potential.[155]

Chapter 5

Conclusions

The forces governing the long-range interactions between molecules are significantly different from their short-ranged counterparts. The latter are due to the Pauli exclusion principle, which prohibits electrons with the same spin from occupying the space where the electron clouds of the interacting molecules overlap. The electron density in this region is thus diminished, and the incompletely shielded nuclei exert a repulsive force on each other.[101] When the overlap of the electron densities is small, the long-range components of the intermolecular forces become significant. Based on physical origin, they divide into three components, of which only one, the London dispersion force, is present in all molecular interactions. This force plays an instrumental part in a host of phenomena,[2–14] and for simple molecules, it is often the greatest contributor to the long-range attractive force.[16,101]

The approach adopted in this thesis for the study of long-range forces relies on the perturbative series expansion of the intermolecular interaction potential, known as the polarization expansion.[85,86] Furthermore, the Coulombic potentials of the participating molecules are expanded in terms of electric multipole moments and polarizabilities, which enable the description of the intermolecular forces solely in terms of monomer properties. In Chapter 3 it is shown how the different long-range contributions to the energy naturally emerge as different levels of perturbation, and their characteristics and properties are discussed.

The research articles included in this thesis are centered around the dispersion interactions present between small clusters of coinage (Cu, Ag, and Au) and volatile (Zn, Cd, and Hg) metals. A computational model is presented to quantify these forces, and its properties and performance are explored in several articles. The *ab initio* calculated dispersion energy is partitioned into pair contributions, and the interaction coefficients describing their magnitudes are extracted from small model clusters. The determined coefficients depend on the geometry of the system, and in Article III they are found to model the dispersion interactions more accurately than the corresponding isotropic parameters. The results obtained for the orientation averaged dispersion energy, and the volatile metal clusters of Article III indicate that the method introduced is viable, and capable of accurately accounting for the London forces in the studied systems.

In Article IV, the long-range interactions are approached from a more theoretical standpoint. A novel formula is derived for the tensor describing the intermolecular forces, and it is applied to examine the coinage metal–hydrogen clusters. The presented equation is based on concepts drawn from combinatorial analysis and the geometric Clifford algebra, and it allows the convenient vector-based description of all kinds of long-range intermolecular forces, as attested by the several exemplary

applications included in Article IV.

On the whole, the theoretical aspects summarized in this thesis, along with the reviewed literature provide an overview of the most important factors affecting the intermolecular interactions at long distances. These considerations serve as a foundation upon which the included research articles are built, describing the application of the elaborated principles to the quantitative modeling of the of non-covalent interactions in the studied clusters. The results have confirmed that the ideas presented in this thesis can be used to construct a simple yet effective method to gauge the dispersion interactions, and incorporate them as a contribution to the total interaction energy. This type of procedure, along with the results obtained, should be especially interesting for the modeling of the London forces in large systems where the dispersion interactions can be decisive, but highly correlated electronic structure methods are unfeasible. For the pair-potential model presented in this thesis, no experimental parameters are required, and after the dispersion coefficients have been recovered, no additional electronic structure calculations are necessary.

Bibliography

[1] van der Waals, J. D. Thermodynamische Theorie der Capillariteit in de Onderstelling van Continue Dichtheidsverandering [The Thermodynamic Theory of Capillarity under the Hypothesis of a Continuous Variation of Density]. *Verhand. Konink. Akad. Weten. Amsterdam (Sect. 1)* **1893**, *1, No. 8*, 1–56, DOI: 10.1007/BF01011514, Translation by Rowlinson, J. S. *J. Stat. Phys.* **1979**, *20*, 200–244.

[2] Autumn, K.; Sitti, M.; Liang, Y. A.; Peattie, A. M.; Hansen, W. R.; Sponberg, S.; Kenny, T. W.; Fearing, R.; Israelachvili, J. N.; Full, R. J. Evidence for van der Waals Adhesion in Gecko Setae. *Proc. Natl. Acad. Sci. U. S. A.* **2002**, *99*, 12252–12256, DOI: 10.1073/pnas.192252799.

[3] Kesel, A. B.; Martin, A.; Seidl, T. Getting a Grip on Spider Attachment: an AFM Approach to Microstructure Adhesion in Arthropods. *Smart Mater. Struct.* **2004**, *13*, 512–518, DOI: 10.1088/0964-1726/13/3/009.

[4] Lau, K. A.; Messersmith, P. B. In *Biological Adhesive Systems*; von Byern, J., Grunwald, I., Eds.; Springer Vienna, 2010; pp 285–294, DOI: 10.1007/978-3-7091-0286-2_19.

[5] Wolff, J. O.; Gorb, S. N. The Influence of Humidity on the Attachment Ability of the Spider Philodromus Dispar (Araneae, Philodromidae). *Proc. R. Soc. B* **2011**, *279*, 139–143, DOI: 10.1098/rspb.2011.0505.

[6] Swamy, K. S. K. *Dust in the Universe*; World Scientific Series in Astronomy and Astrophysics; World Scientific Publishing Co. Pte. Ltd., Singapore, 2005; Vol. 7; DOI: 10.1142/9789812567666_0002.

[7] Wright, J. D. *Molecular Crystals*, 2nd ed.; Cambridge University Press, Wiltshire, 1995.

[8] Björkman, T.; Gulans, A.; Krasheninnikov, A. V.; Nieminen, R. M. van der Waals Bonding in Layered Compounds from Advanced Density-Functional First-Principles Calculations. *Phys. Rev. Lett.* **2012**, *108*, 235502, DOI: 10.1103/PhysRevLett.108.235502.

[9] Gao, G. et al. Artificially Stacked Atomic Layers: Toward New van der Waals Solids. *Nano Lett.* **2012**, *12*, 3518–3525, DOI: 10.1021/nl301061b.

[10] Geim, A. K.; Grigorieva, I. V. Van der Waals Heterostructures. *Nature* **2013**, *499*, 419–425, DOI: 10.1038/nature12385.

[11] Hobza, P.; Šponer, J. Structure, Energetics, and Dynamics of the Nucleic Acid Base Pairs: Nonempirical *ab Initio* Calculations. *Chem. Rev.* **1999**, *99*, 3247–3276, DOI: 10.1021/cr9800255.

[12] Černý, J.; Kabeláč, M.; Hobza, P. Double-Helical → Ladder Structural Transition in the B-DNA is Induced by a Loss of Dispersion Energy. *J. Am. Chem. Soc.* **2008**, *130*, 16055–16059, DOI: 10.1021/ja805428q.

[13] Hobza, P.; Müller-Dethlefs, K. *Non-Covalent Interactions: Theory and Experiment*; RSC Theoretical and Computational Chemistry Series; The Royal Society of Chemistry, Cambridge, 2010; Vol. 2; DOI: 10.1039/9781847559906.

[14] Riley, K. E.; Hobza, P. Noncovalent Interactions in Biochemistry. *Wiley Interdiscip. Rev.: Comput. Mol. Sci.* **2011**, *1*, 3–17, DOI: 10.1002/wcms.8.

[15] London, F. The General Theory of Molecular Forces. *Trans. Faraday Soc.* **1937**, *33*, 8–26, DOI: 10.1039/TF937330008B.

[16] Israelachvili, J. N. *Intermolecular and Surface Forces*, 3rd ed.; Academic Press, San Diego, 2011; DOI: 10.1016/B978-0-12-375182-9.10006-5.

[17] London, F. Zur Theorie und Systematik der Molekularkräfte [On the Theory and System of Molecular Forces]. *Z. Phys.* **1930**, *63*, 245–279, DOI: 10.1007/BF01421741, Translation by Hettema, H. In *Quantum Chemistry : Classic Scientific Papers*; Hettema, H., Ed.; World Scientific Publishing Co. Pte. Ltd., Singapore, 2000; pp 369–399, DOI: 10.1142/9789812795762_0023.

[18] Béguin, L.; Vernier, A.; Chicireanu, R.; Lahaye, T.; Browaeys, A. Direct Measurement of the van der Waals Interaction between Two Rydberg Atoms. *Phys. Rev. Lett.* **2013**, *110*, 263201, DOI: 10.1103/PhysRevLett.110.263201.

[19] Weidemüller, M. Viewpoint: Atomic Interactions at a Distance. *Physics* **2013**, *6*, 71, DOI: 10.1103/Physics.6.71.

[20] Alonso, J.; Mañanes, A. Long-Range van der Waals Interactions in Density Functional Theory. *Theor. Chem. Acc.* **2007**, *117*, 467–472, DOI: 10.1007/s00214-006-0079-3.

[21] Burke, K. Perspective on Density Functional Theory. *J. Chem. Phys.* **2012**, *136*, 150901, DOI: 10.1063/1.4704546.

[22] Cohen, A. J.; Mori-Sánchez, P.; Yang, W. Challenges for Density Functional Theory. *Chem. Rev.* **2012**, *112*, 289–320, DOI: 10.1021/cr200107z.

[23] Klimeš, J.; Michaelides, A. Perspective: Advances and Challenges in Treating van der Waals Dispersion Forces in Density Functional Theory. *J. Chem. Phys.* **2012**, *137*, 120901, DOI: 10.1063/1.4754130.

[24] Waller, M.; Grimme, S. In *Handbook of Computational Chemistry*; Leszczynski, J., Ed.; Springer Netherlands, 2014; pp 443–466, DOI: 10.1007/978-94-007-0711-5_12.

[25] Elstner, M.; Hobza, P.; Frauenheim, T.; Suhai, S.; Kaxiras, E. Hydrogen Bonding and Stacking Interactions of Nucleic Acid Base Pairs: A Density-Functional-Theory Based Treatment. *J. Chem. Phys.* **2001**, *114*, 5149–5155, DOI: 10.1063/1.1329889.

[26] Korona, T.; Przybytek, M.; Jeziorski, B. Time-Independent Coupled Cluster Theory of the Polarization Propagator. Implementation and Application of the Singles and Doubles Model to Dynamic Polarizabilities and van der Waals Constants. *Mol. Phys.* **2006**, *104*, 2303–2316, DOI: 10.1080/00268970600673975.

[27] Grimme, S. Semiempirical GGA-type Density Functional Constructed with a Long-Range Dispersion Correction. *J. Comput. Chem.* **2006**, *27*, 1787–1799, DOI: 10.1002/jcc.20495.

[28] Tkatchenko, A.; Scheffler, M. Accurate Molecular van der Waals Interactions from Ground-State Electron Density and Free-Atom Reference Data. *Phys. Rev. Lett.* **2009**, *102*, 073005, DOI: 10.1103/PhysRevLett.102.073005.

[29] Grimme, S.; Antony, J.; Ehrlich, S.; Krieg, H. A Consistent and Accurate ab Initio Parametrization of Density Functional Dispersion Correction (DFT-D) for the 94 Elements H-Pu. *J. Chem. Phys.* **2010**, *132*, 154104, DOI: 10.1063/1.3382344.

[30] Norman, P. A Perspective on Nonresonant and Resonant Electronic Response Theory for Time-Dependent Molecular Properties. *Phys. Chem. Chem. Phys.* **2011**, *13*, 20519–20535, DOI: 10.1039/C1CP21951K.

[31] Zhang, G.-X.; Tkatchenko, A.; Paier, J.; Appel, H.; Scheffler, M. van der Waals Interactions in Ionic and Semiconductor Solids. *Phys. Rev. Lett.* **2011**, *107*, 245501, DOI: 10.1103/PhysRevLett.107.245501.

[32] Szalewicz, K. Symmetry-Adapted Perturbation Theory of Intermolecular Forces. *Wiley Interdiscip. Rev.: Comput. Mol. Sci.* **2012**, *2*, 254–272, DOI: 10.1002/wcms.86.

[33] Tkatchenko, A.; DiStasio, R. A.; Car, R.; Scheffler, M. Accurate and Efficient Method for Many-Body van der Waals Interactions. *Phys. Rev. Lett.* **2012**, *108*, 236402, DOI: 10.1103/PhysRevLett.108.236402.

[34] Jansen, G. Symmetry-Adapted Perturbation Theory Based on Density Functional Theory for Noncovalent Interactions. *Wiley Interdiscip. Rev.: Comput. Mol. Sci.* **2014**, *4*, 127–144, DOI: 10.1002/wcms.1164.

[35] Schmidbaur, H. The Aurophilicity Phenomenon: A Decade of Experimental Findings, Theoretical Concepts and Emerging Applications. *Gold Bull.* **2000**, *33*, 3–10, DOI: 10.1007/bf03215477.

[36] Schmidbaur, H.; Schier, A. A Briefing on Aurophilicity. *Chem. Soc. Rev.* **2008**, *37*, 1931–1951, DOI: 10.1039/b708845k.

[37] Sculfort, S.; Braunstein, P. Intramolecular d^{10}–d^{10} Interactions in Heterometallic Clusters of the Transition Metals. *Chem. Soc. Rev.* **2011**, *40*, 2741–2760, DOI: 10.1039/c0cs00102c.

[38] Schmidbaur, H.; Schier, A. Aurophilic Interactions as a Subject of Current Research: an Up-Date. *Chem. Soc. Rev.* **2012**, *41*, 370–412, DOI: 10.1039/c1cs15182g.

[39] Otero-de-la Roza, A.; Mallory, J. D.; Johnson, E. R. Metallophilic Interactions from Dispersion-Corrected Density-Functional Theory. *J. Chem. Phys.* **2014**, *140*, 18A504, DOI: 10.1063/1.4862896.

[40] de Heer, W. A. The Physics of Simple Metal Clusters: Experimental Aspects and Simple Models. *Rev. Mod. Phys.* **1993**, *65*, 611–676, DOI: 10.1103/RevModPhys.65.611.

[41] Flad, H.-J.; Schautz, F.; Wang, Y.; Dolg, M.; Savin, A. On the Bonding of Small Group 12 Clusters. *Eur. Phys. J. D* **1999**, *6*, 243–254, DOI: 10.1007/PL00021622.

[42] Zhao, J. Density-Functional Study of Structures and Electronic Properties of Cd Clusters. *Phys. Rev. A: At., Mol., Opt. Phys.* **2001**, *64*, 043204, DOI: 10.1103/PhysRevA.64.043204.

[43] Moyano, G. E.; Wesendrup, R.; Söhnel, T.; Schwerdtfeger, P. Properties of Small- to Medium-Sized Mercury Clusters from a Combined ab Initio, Density-Functional, and Simulated-Annealing Study. *Phys. Rev. Lett.* **2002**, *89*, 103401, DOI: 10.1103/PhysRevLett.89.103401.

[44] Wang, J.; Wang, G.; Zhao, J. Nonmetal-Metal Transition in Zn_n ($n = 2 - 20$) Clusters. *Phys. Rev. A: At., Mol., Opt. Phys.* **2003**, *68*, 013201, DOI: 10.1103/PhysRevA.68.013201.

[45] Gaston, N.; Schwerdtfeger, P. From the van der Waals Dimer to the Solid State of Mercury with Relativistic *ab Initio* and Density Functional Theory. *Phys. Rev. B: Condens. Matter Mater. Phys.* **2006**, *74*, 024105, DOI: 10.1103/PhysRevB.74.024105.

[46] Born, M.; Oppenheimer, R. Zur Quantentheorie der Molekeln [On the Quantum Theory of Molecules]. *Ann. Phys.* **1927**, *389*, 457–484, DOI: 10.1002/andp.19273892002, Translation by Hettema, H. In *Quantum Chemistry : Classic Scientific Papers*; Hettema, H., Ed.; World Scientific Publishing Co. Pte. Ltd., Singapore, 2000; pp 1–24, DOI: 10.1142/9789812795762_0001.

[47] Ritz, W. Über eine Neue Methode zur Lösung Gewisser Variationsprobleme der Mathematischen Physik [A New Method of Solving Certain Variational Problems of Mathematical Physics]. *J. Reine Angew. Math.* **1909**, *1909*, 1–61, DOI: 10.1515/crll.1909.135.1.

[48] Szabo, A.; Ostlund, N. S. *Modern Quantum Chemistry: Introduction to Advanced Electronic Structure Theory*; Dover Publications, Inc., Mineola, New York, 1996.

[49] Dinur, U. In *Encyclopedia of Computational Chemistry*; von Ragué Schleyer, P., Allinger, N. L., Clark, T., Gasteiger, J., Kollman, P. A., Schaefer, H. F., Schreiner, P. R., Eds.; John Wiley & Sons Ltd, Chichester, 1998; Vol. 1; pp 264–271, DOI: 10.1002/0470845015.cca012.

[50] Hellmann, H. *Einführung in die Quantenchemie [Introduction to Quantum Chemistry]*; Franz Deuticke, Leipzig, 1937; DOI: 10.1007/978-3-662-45967-6, Reprinted in *Hans Hellmann: Einführung in die Quantenchemie*; Andrae, D., Ed.; Springer, Berlin, 2015; pp 19–376.

[51] Feynman, R. P. Forces in Molecules. *Phys. Rev.* **1939**, *56*, 340–343, DOI: 10.1103/PhysRev.56.340.

[52] Carfì, D. The Pointwise Hellmann–Feynman Theorem. *Atti Accad. Peloritana Pericolanti, Cl. Sci. Fis., Mat. Nat.* **2010**, *88*, C1A1001004, DOI: 10.1478/C1A1001004.

[53] Jensen, F. *Introduction to Computational Chemistry*, 2nd ed.; John Wiley & Sons, Chichester, 2007.

[54] Dirac, P. A. M. On the Theory of Quantum Mechanics. *Proc. R. Soc. A* **1926**, *112*, 661–677, DOI: 10.1098/rspa.1926.0133.

[55] Slater, J. C. The Theory of Complex Spectra. *Phys. Rev.* **1929**, *34*, 1293–1322, DOI: 10.1103/PhysRev.34.1293.

[56] Lewars, E. G. *Computational Chemistry. Introduction to the Theory and Applications of Molecular and Quantum Mechanics*; Springer Netherlands, 2011; DOI: 10.1007/978-90-481-3862-3.

[57] Bransden, B. H.; Joachain, C. J. *Quantum Mechanics*, 2nd ed.; Prentice Hall, Harlow, England, 2000.

[58] Brillouin, L. *La Méthode du Champ Self-Consistent [The Self-Consistent Field Method]*; Actualités Scientifiques et Industrielles [Current Scientific and Industrial Topics]; Hermann & Cie, Paris, 1933; Vol. 71.

[59] Helgaker, T.; Jørgensen, P.; Olsen, J. *Molecular Electronic-Structure Theory*; John Wiley & Sons, Chichester, 2000.

[60] Møller, C.; Plesset, M. S. Note on an Approximation Treatment for Many-Electron Systems. *Phys. Rev.* **1934**, *46*, 618–622, DOI: 10.1103/PhysRev.46.618.

[61] Magnasco, V. *Elementary Methods of Molecular Quantum Mechanics*; Elsevier B. V., Amsterdam, 2007; DOI: 10.1016/b978-044452778-3/50021-9.

[62] Pyykkö, P. Relativistic Effects in Structural Chemistry. *Chem. Rev.* **1988**, *88*, 563–594, DOI: 10.1021/cr00085a006.

[63] Pyykkö, P. Relativistic Effects in Chemistry: More Common Than You Thought. *Annu. Rev. Phys. Chem.* **2012**, *63*, 45–64, DOI: 10.1146/annurev-physchem-032511-143755.

[64] Cao, X.; Dolg, M. Pseudopotentials and Modelpotentials. *Wiley Interdiscip. Rev.: Comput. Mol. Sci.* **2011**, *1*, 200–210, DOI: 10.1002/wcms.28.

[65] Dolg, M.; Cao, X. Relativistic Pseudopotentials: Their Development and Scope of Applications. *Chem. Rev.* **2012**, *112*, 403–480, DOI: 10.1021/cr2001383.

[66] Casimir, H. B. G.; Polder, D. The Influence of Retardation on the London–van der Waals Forces. *Phys. Rev.* **1948**, *73*, 360–372, DOI: 10.1103/PhysRev.73.360.

[67] Greiner, W. *Classical Electrodynamics*; Classical Theoretical Physics; Springer-Verlag, New York, 1998; DOI: 10.1007/978-1-4612-0587-6.

[68] Applequist, J. Traceless Cartesian Tensor Forms for Spherical Harmonic Functions: New Theorems and Applications to Electrostatics of Dielectric Media. *J. Phys. A: Math. Gen.* **1989**, *22*, 4303–4330, DOI: 10.1088/0305-4470/22/20/011.

[69] Vigné-Maeder, F.; Claverie, P. The Exact Multicenter Multipolar Part of a Molecular Charge Distribution and Its Simplified Representations. *J. Chem. Phys.* **1988**, *88*, 4934–4948, DOI: 10.1063/1.454705.

[70] Stone, A. J. *The Theory of Intermolecular Forces*, 2nd ed.; Oxford University Press, Oxford, 2013; DOI: 10.1093/acprof:oso/9780199672394.001.0001.

[71] Zangwill, A. *Modern Electrodynamics*; Cambridge University Press, Cambridge, 2013.

[72] Tough, R. J. A.; Stone, A. J. Properties of the Regular and Irregular Solid Harmonics. *J. Phys. A: Math. Gen.* **1977**, *10*, 1261–1269, DOI: 10.1088/0305-4470/10/8/004.

[73] Axler, S.; Bourdon, P.; Ramey, W. *Harmonic Function Theory*; Graduate Texts in Mathematics; Springer, New York, 2001; Vol. 137; DOI: 10.1007/978-1-4757-8137-3.

[74] Stanley, R. P. *Enumerative Combinatorics, Volume 1*, 2nd ed.; Cambridge Studies in Advanced Mathematics; Cambridge University Press, 2012; Vol. 49.

[75] Arfken, G. B.; Weber, H. J.; Harris, F. E. *Mathematical Methods for Physicists*, 7th ed.; Academic Press, Waltham, 2013; DOI: 10.1016/b978-0-12-384654-9.00016-5.

[76] Brink, D. M.; Satchler, G. R. *Angular Momentum*, 3rd ed.; Clarendon Press, Oxford, 1993.

[77] Hättig, C.; Heß, B. A. Calculation of Orientation-Dependent Double-Tensor Moments for Coulomb-Type Intermolecular Interactions. *Mol. Phys.* **1994**, *81*, 813–824, DOI: 10.1080/00268979400100541.

[78] Schwerdtfeger, P. In *Atoms, Molecules and Clusters in Electric Fields: Theoretical Approaches to the Calculation of Electric Polarizability*; Maroulis, G., Ed.; Series in Computational, Numerical and Mathematical Methods in Sciences and Engineering; World Scientific Publishing Co. Pte. Ltd., Singapore, 2006; Vol. 1; Chapter Atomic Static Dipole Polarizabilities, pp 1–32, DOI: 10.1142/9781860948862_0001.

[79] Bishop, D. M. Molecular Vibrational and Rotational Motion in Static and Dynamic Electric Fields. *Rev. Mod. Phys.* **1990**, *62*, 343–374, DOI: 10.1103/revmodphys.62.343.

[80] Buckingham, A. D. In *Intermolecular Forces*; Hirschfelder, J. O., Ed.; Advances in Chemical Physics; John Wiley & Sons, Inc., 1967; Vol. 12; Chapter Permanent and Induced Molecular Moments and Long-Range Intermolecular Forces, pp 107–142, DOI: 10.1002/9780470143582.ch2.

[81] Elking, D. M.; Perera, L.; Duke, R.; Darden, T.; Pedersen, L. G. A Finite Field Method for Calculating Molecular Polarizability Tensors for Arbitrary Multipole Rank. *J. Comput. Chem.* **2011**, *32*, 3283–3295, DOI: 10.1002/jcc.21914.

[82] van der Avoird, A.; Wormer, P. E. S.; Mulder, F.; Berns, R. M. *Van der Waals Systems*; Topics in Current Chemistry; Springer Berlin Heidelberg, 1980; Vol. 93; pp 1–51, DOI: 10.1007/3-540-10058-X_7.

[83] Buckingham, A. D.; Fowler, P. W.; Hutson, J. M. Theoretical Studies of van der Waals Molecules and Intermolecular Forces. *Chem. Rev.* **1988**, *88*, 963–988, DOI: 10.1021/cr00088a008.

[84] Schrödinger, E. Quantisierung als Eigenwertproblem. Dritte Mitteilung: Störungstheorie mit Anwendung auf den Starkeffekt der Balmerlinien [Quantisation as a Problem of Proper Values. Part III: Perturbation Theory, with Application to the Stark Effect of the Balmer Lines]. *Ann. Phys.* **1926**, *385*, 437–490, DOI: 10.1002/andp.19263851302, Translation by Shearer, J. F. and Deans, W. M. In *Collected Papers on Wave Mechanics*; Blackie & Son Ltd., London, 1928; pp 62–101.

[85] Hirschfelder, J. Perturbation Theory for Exchange Forces, I. *Chem. Phys. Lett.* **1967**, *1*, 325–329, DOI: 10.1016/0009-2614(67)80007-1.

[86] Hirschfelder, J. Perturbation Theory for Exchange Forces, II. *Chem. Phys. Lett.* **1967**, *1*, 363–368, DOI: 10.1016/0009-2614(67)80036-8.

[87] Stogryn, D. E. Higher Order Interaction Energies for Systems of Asymmetric Molecules. *Mol. Phys.* **1971**, *22*, 81–103, DOI: 10.1080/00268977100102361.

[88] Piecuch, P. Spherical Tensor Theory of Long-Range Interactions in a System of N Arbitrary Molecules Including Quantum-Mechanical Many-Body Effects I. Anisotropic Induction Interactions in the First Three Orders of Perturbation Theory. *Mol. Phys.* **1986**, *59*, 1067–1083, DOI: 10.1080/00268978600102591.

[89] Piecuch, P. Spherical Tensor Theory of Long-Range Interactions in a System of N Arbitrary Molecules Including Quantum-Mechanical Many-Body Effects II. Anisotropic Dispersion Interactions in the First Three Orders of Perturbation Theory. *Mol. Phys.* **1986**, *59*, 1085–1095, DOI: 10.1080/00268978600102601.

[90] Piecuch, P. Spherical Tensor Theory of Long-Range Interactions in a System of N Arbitrary Molecules Including Quantum-Mechanical Many-Body Effects III. Isotropic Interactions in the First Three Orders of Perturbation Theory. *Mol. Phys.* **1986**, *59*, 1097–1111, DOI: 10.1080/00268978600102611.

[91] Jeziorski, B.; Moszynski, R.; Szalewicz, K. Perturbation Theory Approach to Intermolecular Potential Energy Surfaces of van der Waals Complexes. *Chem. Rev.* **1994**, *94*, 1887–1930, DOI: 10.1021/cr00031a008.

[92] Moszynski, R.; Wormer, P. E. S.; Jeziorski, B.; van der Avoird, A. Symmetry-Adapted Perturbation Theory of Nonadditive Three-Body Interactions in van der Waals Molecules. I. General Theory. *J. Chem. Phys.* **1995**, *103*, 8058–8074, DOI: 10.1063/1.470171, *Erratum*: *J. Chem. Phys.* **1997**, *107*, 672–673.

[93] Patkowski, K.; Szalewicz, K.; Jeziorski, B. Third-Order Interactions in Symmetry-Adapted Perturbation Theory. *J. Chem. Phys.* **2006**, *125*, 154107, DOI: 10.1063/1.2358353.

[94] Brooks, F. C. Convergence of Intermolecular Force Series. *Phys. Rev.* **1952**, *86*, 92–97, DOI: 10.1103/PhysRev.86.92.

[95] Claverie, P. Theory of Intermolecular Forces. I. On the Inadequacy of the Usual Rayleigh–Schrödinger Perturbation Method for the Treatment of Intermolecular Forces. *Int. J. Quantum Chem.* **1971**, *5*, 273–296, DOI: 10.1002/qua.560050304.

[96] Ahlrichs, R. Convergence Properties of the Intermolecular Force Series (1/R-Expansion). *Theor. Chim. Acta* **1976**, *41*, 7–15, DOI: 10.1007/BF00558020.

[97] Chałasiński, G.; Jeziorski, B.; Szalewicz, K. On the Convergence Properties of the Rayleigh–Schrödinger and the Hirschfelder–Silbey Perturbation Expansions for Molecular Interaction Energies. *Int. J. Quantum Chem.* **1977**, *11*, 247–257, DOI: 10.1002/qua.560110205.

[98] Kutzelnigg, W. The “Primitive" Wave Function in the Theory of Intermolecular Interactions. *J. Chem. Phys.* **1980**, *73*, 343–359, DOI: 10.1063/1.439880.

[99] Adams, W. H. On the Limits of Validity of the Symmetrized Rayleigh–Schrödinger Perturbation Theory. *Int. J. Quantum Chem.* **1996**, *60*, 273–285, DOI: 10.1002/(SICI)1097-461X(1996)60:1<273::AID-QUA28>3.0.CO;2-E.

[100] Patkowski, K.; Korona, T.; Jeziorski, B. Convergence Behavior of the Symmetry-Adapted Perturbation Theory for States Submerged in Pauli Forbidden Continuum. *J. Chem. Phys.* **2001**, *115*, 1137–1152, DOI: 10.1063/1.1379330.

[101] Maitland, G. C.; Rigby, M.; Smith, E. B.; Wakeham, W. A. *Intermolecular Forces: Their Origin and Determination*; International Series of Monographs on Chemistry; Clarendon Press, Oxford, 1981; Vol. 3.

[102] Kaplan, I. G. *Intermolecular Interactions: Physical Picture, Computational Methods and Model Potentials*; John Wiley & Sons Ltd, Chichester, 2006; DOI: 10.1002/047086334x.

[103] Axilrod, B. M.; Teller, E. Interaction of the van der Waals Type between Three Atoms. *J. Chem. Phys.* **1943**, *11*, 299–300, DOI: 10.1063/1.1723844.

[104] Muto, Y. 非極性分子の間に作用する力に就いて [The Force between Nonpolar Molecules]. 日本数学物理学会誌 *[J. Phys.-Math. Soc. Japan]* **1943**, *17*, 629–631, DOI: 10.11429/subutsukaishi1927.17.10-11-12_629.

[105] Bell, R. J. Multipolar Expansion for the Non-Additive Third-Order Interaction Energy of Three Atoms. *J. Phys. B: At. Mol. Phys.* **1970**, *3*, 751–762, DOI: 10.1088/0022-3700/3/6/003.

[106] Doran, M. B.; Zucker, I. J. Higher Order Multipole Three-Body van der Waals Interactions and Stability of Rare Gas Solids. *J. Phys. C: Solid State Phys.* **1971**, *4*, 307–312, DOI: 10.1088/0022-3719/4/3/006.

[107] Tang, L.-Y.; Yan, Z.-C.; Shi, T.-Y.; Babb, J. F.; Mitroy, J. The Long-range Non-Additive Three-Body Dispersion Interactions for the Rare Gases, Alkali, and Alkaline-Earth Atoms. *J. Chem. Phys.* **2012**, *136*, 104104, DOI: 10.1063/1.3691891.

[108] Stone, A. Distributed Multipole Analysis, or How to Describe a Molecular Charge Distribution. *Chem. Phys. Lett.* **1981**, *83*, 233–239, DOI: 10.1016/0009-2614(81)85452-8.

[109] Sokalski, W. A.; Poirier, R. A. Cumulative Atomic Multipole Representation of the Molecular Charge Distribution and its Basis Set Dependence. *Chem. Phys. Lett.* **1983**, *98*, 86–92, DOI: 10.1016/0009-2614(83)80208-5.

[110] Stone, A. J.; Alderton, M. Distributed Multipole Analysis. Methods and Applications. *Mol. Phys.* **1985**, *56*, 1047–1064, DOI: 10.1080/00268978500102891.

[111] Kielich, S.; Zawodny, R. Tensor Elements of the Molecular Electric Multipole Moments for all Point Group Symmetries. *Chem. Phys. Lett.* **1971**, *12*, 20–24, DOI: 10.1016/0009-2614(71)80607-3.

[112] Gelessus, A.; Thiel, W.; Weber, W. Multipoles and Symmetry. *J. Chem. Educ.* **1995**, *72*, 505–508, DOI: 10.1021/ed072p505.

[113] Stone, A. J.; Tough, R. J. A. Spherical Tensor Theory of Long-Range Intermolecular Forces. *Chem. Phys. Lett.* **1984**, *110*, 123–129, DOI: 10.1016/0009-2614(84)80160-8.

[114] Pantaleone, J. Synchronization of Metronomes. *Am. J. Phys.* **2002**, *70*, 992–1000, DOI: 10.1119/1.1501118.

[115] Drude, P. *The Theory of Optics*; Longmans, Green, and Co., New York, 1902.

[116] Heisenberg, W. Über Quantentheoretische Umdeutung Kinematischer und Mechanischer Beziehungen. [Quantum-Theoretical Re-Interpretation of Kinematic and Mechanical Relations]. *Z. Physik* **1925**, *33*, 879–893, DOI: 10.1007/BF01328377, Translation in *Sources of Quantum Mechanics*; van der Waerden, B. L., Ed.; North-Holland Publishing Co., Amsterdam, 1967; pp 261–276.

[117] Heisenberg, W. Über den Anschaulichen Inhalt der Quantentheoretischen Kinematik und Mechanik [The Physical Content of Quantum Kinematics and Mechanics]. *Z. Phys.* **1927**, *43*, 172–198, DOI: 10.1007/BF01397280, Translation by Wheeler, J. A. and Zurek, W. H. In *Quantum Theory and Measurement*; Wheeler, J. A. and Zurek, W. H., Eds.; Princeton University Press, Princeton, New Jersey, 1983; pp 62–86.

[118] Green, S. Rotational Excitation in H_2–H_2 Collisions: Close-Coupling Calculations. *J. Chem. Phys.* **1975**, *62*, 2271, DOI: 10.1063/1.430752.

[119] Burton, P. G.; Senff, U. E. The $(H_2)_2$ Potential Surface and the Interaction between Hydrogen Molecules at Low Temperatures. *J. Chem. Phys.* **1982**, *76*, 6073, DOI: 10.1063/1.442963.

[120] Diep, P.; Johnson, J. K. An Accurate H_2–H_2 Interaction Potential from First Principles. *J. Chem. Phys.* **2000**, *112*, 4465–4473, DOI: 10.1063/1.481009.

[121] Diep, P.; Johnson, J. K. Erratum: "An Accurate H_2–H_2 Interaction Potential from First Principles" [J. Chem. Phys. 112, 4465 (2000)]. *J. Chem. Phys.* **2000**, *113*, 3480–3481, DOI: 10.1063/1.1287060.

[122] Hardy, M. The Combinatorics of Partial Derivatives. *Electron. J. Comb.* **2006**, *13*, #R1.

[123] Doran, C.; Lasenby, A. *Geometric Algebra for Physicists*; Cambridge University Press, Cambridge, 2005; DOI: 10.1017/CBO9780511807497.

[124] Hestenes, D. *New Foundations for Classical Mechanics*; Springer Netherlands, 2002; DOI: 10.1007/0-306-47122-1.

[125] Mansour, T. In *Combinatorics of Set Partitions*; Rosen, K. H., Ed.; Discrete Mathematics and Its Applications; CRC Press, Boca Raton, FL, 2013; DOI: 10.1201/b12691.

[126] Cohen, H. D.; Roothaan, C. C. J. Electric Dipole Polarizability of Atoms by the Hartree–Fock Method. I. Theory for Closed-Shell Systems. *J. Chem. Phys.* **1965**, *43*, S34–S39, DOI: 10.1063/1.1701512.

[127] Pople, J. A.; McIver Jr., J. A.; Ostlund, N. S. Self-Consistent Perturbation Theory. I. Finite Perturbation Methods. *J. Chem. Phys.* **1968**, *49*, 2960–2964, DOI: 10.1063/1.1670536.

[128] Sauer, S. P. A. *Molecular Electromagnetism: A Computational Chemistry Approach.*; Oxford Graduate Texts; Oxford University Press, Oxford, 2011; DOI: 10.1093/acprof:oso/9780199575398.001.0001.

[129] Kurtz, H. A.; Stewart, J. J. P.; Dieter, K. M. Calculation of the Nonlinear Optical Properties of Molecules. *J. Comput. Chem.* **1990**, *11*, 82–87, DOI: 10.1002/jcc.540110110.

[130] Kobus, J. Hartree–Fock Limit Values of Multipole Moments, Polarizabilities, and Hyperpolarizabilities for Atoms and Diatomic Molecules. *Phys. Rev. A* **2015**, *91*, 022501, DOI: 10.1103/PhysRevA.91.022501.

[131] Mohammed, A. A. K.; Limacher, P. A.; Champagne, B. Finding Optimal Finite Field Strengths Allowing for a Maximum of Precision in the Calculation of Polarizabilities and Hyperpolarizabilities. *J. Comput. Chem.* **2013**, *34*, 1497–1507, DOI: 10.1002/jcc.23285.

[132] Shelton, D. P.; Rice, J. E. Measurements and Calculations of the Hyperpolarizabilities of Atoms and Small Molecules in the Gas Phase. *Chem. Rev.* **1994**, *94*, 3–29, DOI: 10.1021/cr00025a001.

[133] Saue, T.; Jensen, H. J. A. Linear Response at the 4-Component Relativistic Level: Application to the Frequency-Dependent Dipole Polarizabilities of the Coinage Metal Dimers. *J. Chem. Phys.* **2003**, *118*, 522–536, DOI: 10.1063/1.1522407.

[134] Mohr, P. J.; Taylor, B. N.; Newell, D. B. The 2014 CODATA Recommended Values of the Fundamental Physical Constants (Web Version 7.0). National Institute of Standards and Technology, Gaithersburg, Maryland, 2015; This database was developed by J. Baker, M. Douma, and S. Kotochigova. Available: `http://physics.nist.gov/constants`. Retrieved September 17, 2015.

[135] Fornberg, B. Classroom Note:Calculation of Weights in Finite Difference Formulas. *SIAM Rev.* **1998**, *40*, 685–691, DOI: 10.1137/S0036144596322507.

[136] Schautz, F.; Flad, H.-J.; Dolg, M. Quantum Monte Carlo Study of Be_2 and Group 12 Dimers M_2 (M = Zn, Cd, Hg). *Theor. Chem. Acc.* **1998**, *99*, 231–240, DOI: 10.1007/s002140050331.

[137] Schwerdtfeger, P.; Wesendrup, R.; Moyano, G. E.; Sadlej, A. J.; Greif, J.; Hensel, F. The Potential Energy Curve and Dipole Polarizability Tensor of Mercury Dimer. *J. Chem. Phys.* **2001**, *115*, 7401–7412, DOI: 10.1063/1.1402163.

[138] Maroulis, G. Electric Quadrupole Moment and Quadrupole Polarizability of the Copper Dimer from High Level ab Initio and Some Density Functional Theory Calculations. *Comput. Theor. Chem.* **2013**, *1021*, 233–239, DOI: 10.1016/j.comptc.2013.07.038.

[139] Bishop, D. M.; Pipin, J. Dipole, Quadrupole, Octupole, and Dipole-Octupole Polarizabilities at Real and Imaginary Frequencies for H, He, and H_2 and the Dispersion-Energy Coefficients for Interactions between Them. *Int. J. Quantum Chem.* **1993**, *45*, 349–361, DOI: 10.1002/qua.560450403.

[140] Hinde, R. J. Vibrational dependence of the H_2–H_2 C_6 dispersion coefficients. *J. Chem. Phys.* **2005**, *122*, 144304, DOI: 10.1063/1.1873512.

[141] Dunning, T. H. Gaussian Basis Sets for Use in Correlated Molecular Calculations. I. The Atoms Boron through Neon and Hydrogen. *J. Chem. Phys.* **1989**, *90*, 1007–1023, DOI: 10.1063/1.456153.

[142] Kendall, R. A.; Dunning, T. H.; Harrison, R. J. Electron Affinities of the First-Row Atoms Revisited. Systematic Basis Sets and Wave Functions. *J. Chem. Phys.* **1992**, *96*, 6796–6806, DOI: 10.1063/1.462569.

[143] Figgen, D.; Rauhut, G.; Dolg, M.; Stoll, H. Energy-Consistent Pseudopotentials for Group 11 and 12 Atoms: Adjustment to Multi-Configuration Dirac–Hartree–Fock Data. *Chem. Phys.* **2005**, *311*, 227–244, DOI: 10.1016/j.chemphys.2004.10.005, Relativistic Effects in Heavy-Element Chemistry and Physics. In Memoriam Bernd A. Hess (1954-2004).

[144] Peterson, K. A.; Puzzarini, C. Systematically Convergent Basis Sets for Transition Metals. II. Pseudopotential-Based Correlation Consistent Basis Sets for the Group 11 (Cu, Ag, Au) and 12 (Zn, Cd, Hg) Elements. *Theor. Chem. Acc.* **2005**, *114*, 283–296, DOI: 10.1007/s00214-005-0681-9.

[145] Hänninen, V.; Korpinen, M.; Ren, Q.; Hinde, R.; Halonen, L. An ab Initio Study of van der Waals Potential Energy Parameters for Silver Clusters. *J. Phys. Chem. A* **2011**, *115*, 2332–2339, DOI: 10.1021/jp110234n.

[146] Jalkanen, J.-P.; Halonen, M.; Fernández-Torre, D.; Laasonen, K.; Halonen, L. A Computational Study of the Adsorption of Small Ag and Au Nanoclusters on Graphite. *J. Phys. Chem. A* **2007**, *111*, 12317–12326, DOI: 10.1021/jp074969m, PMID: 17973466.

[147] Grimme, S. Improved Second-Order Møller–Plesset Perturbation Theory by Separate Scaling of Parallel- and Antiparallel-Spin Pair Correlation Energies. *J. Chem. Phys.* **2003**, *118*, 9095–9102, DOI: 10.1063/1.1569242.

[148] Piacenza, M.; Grimme, S. Van der Waals Interactions in Aromatic Systems: Structure and Energetics of Dimers and Trimers of Pyridine. *ChemPhysChem* **2005**, *6*, 1554–1558, DOI: 10.1002/cphc.200500100.

[149] Hobza, P.; Selzle, H. L.; Schlag, E. W. Potential Energy Surface for the Benzene Dimer. Results of *ab Initio* CCSD(T) Calculations Show Two Nearly Isoenergetic Structures: T-Shaped and Parallel-Displaced. *J. Phys. Chem.* **1996**, *100*, 18790–18794, DOI: 10.1021/jp961239y.

[150] Sinnokrot, M. O.; Valeev, E. F.; Sherrill, C. D. Estimates of the Ab Initio Limit for π–π Interactions: The Benzene Dimer. *J. Am. Chem. Soc.* **2002**, *124*, 10887–10893, DOI: 10.1021/ja025896h.

[151] Tsuzuki, S.; Honda, K.; Uchimaru, T.; Mikami, M. High-Level ab Initio Computations of Structures and Interaction Energies of Naphthalene Dimers: Origin of Attraction and its Directionality. *J. Chem. Phys.* **2004**, *120*, 647–659, DOI: 10.1063/1.1630953.

[152] Jules, J. L.; Lombardi, J. R. Transition Metal Dimer Internuclear Distances from Measured Force Constants. *J. Phys. Chem. A* **2003**, *107*, 1268–1273, DOI: 10.1021/jp027493+.

[153] Seth, M.; Schwerdtfeger, P.; Dolg, M. The Chemistry of the Superheavy Elements. I. Pseudopotentials for 111 and 112 and Relativistic Coupled Cluster Calculations for $(112)H^+$, $(112)F_2$, and $(112)F_4$. *J. Chem. Phys.* **1997**, *106*, 3623–3632, DOI: 10.1063/1.473437.

[154] Pahl, E.; Figgen, D.; Thierfelder, C.; Peterson, K. A.; Calvo, F.; Schwerdtfeger, P. A Highly Accurate Potential Energy Curve for the Mercury Dimer. *J. Chem. Phys.* **2010**, *132*, 114301, DOI: 10.1063/1.3354976.

[155] Tang, K.; Toennies, J. The Dynamical Polarisability and van der Waals Dimer Potential of Mercury. *Mol. Phys.* **2008**, *106*, 1645–1653, DOI: 10.1080/00268970802270059.